

**VALIDATION OF WATER VAPOR MEASUREMENTS FROM COMMERCIAL
AIRCRAFT ACROSS THE CONUS USING RADIOSONDES**

SKYLAR S. WILLIAMS

A thesis submitted in partial fulfillment of

the requirements for the degree of

MASTER OF SCIENCE

(Atmospheric and Oceanic Sciences)

at the

UNIVERSITY OF WISCONSIN-MADISON

2017

Thesis Declaration and Approval

I, Skylar S. Williams, declare that this thesis titled ‘Validation of Water Vapor Measurements from Commercial Aircraft Across the CONUS using Radiosondes’ and the work presented in it are my own.

<u>Skylar S. Williams</u>	_____	_____
Author	Signature	Date

I hereby approve and recommend for acceptance this work in partial fulfillment of the requirements for the degree of Master of Science:

<u>Steven A. Ackerman</u>	_____	_____
Committee Chair	Signature	Date

<u>Grant Petty</u>	_____	_____
Faculty Member	Signature	Date

<u>Ankur Desai</u>	_____	_____
Faculty Member	Signature	Date

Abstract

National Weather Service (NWS) radiosondes are a significant part of the upper-level observing network; however, the limited spatial and temporal coverage of these observations create large gaps in our characterization of the atmosphere. Observations from commercial aircraft are one way to increase the number of observations and fill in data between radiosonde sites. These aircraft data are collected in real-time by the Aircraft Meteorological Data Reports (AMDAR) system and traditionally have contained observations of temperature, wind, and pressure.

In the past, water vapor observations have not been collected since separate instrumentation was required and these observations were not required in-flight for aircraft observations. The development and deployment of the Water Vapor Sensing System II (WVSS-II) on select commercial aircraft have allowed water vapor measurements to be added to this data set. This sensor was designed to be lightweight, require little maintenance, and be highly reliable. Vertical profiles of moisture are provided by the WVSS-II observations during takeoff and landing, yielding complete thermodynamic and kinematic profiles of the atmosphere at higher frequencies than by radiosondes alone.

Radiosonde-based validation of the WVSS-II has been limited to short-term field studies in climatologically similar regions, which limits characterization of its performance in different environments. In the present study, the WVSS-II is compared to operational NWS radiosondes throughout the continental United States, covering all seasons and multiple climate regimes. Locational and seasonal biases are explored, and the performance of the sensor in both high and low water vapor environments is determined. In general, the WVSS-

II is slightly moister than the radiosondes with very little difference between aircraft type.

The summertime tends to have the largest difference while winter has the least. A larger moisture difference was found when examining aircraft flying through precipitation that could be due to moisture being trapped in the air sampler. Characterizing potential biases in the WVSS-II dataset will improve data assimilation processes of this data into numerical weather prediction models and create confidence for both governmental and aviation forecasters regardless of location or time of year.

Acknowledgements

I came to Madison at the end of June of 2015 from Oklahoma where it was in the mid-upper 90's. Madison was in the upper 60's and I froze. All summer. All I could think was "how am I going to survive winter?". Well, good news for me, I survived. I survived all the coursework, research, and the cold to finish this degree but I couldn't do it without the amazing people in my life.

I would like to thank Tim Wagner, my advisor and fellow OU grad, for guiding me on this research. Thank you for throwing me into a project that I didn't even know existed and that I came to love. I had never worked with Matlab for more than one assignment and you had so much patience with me and I've learned so much. Also thank you for talking OU football with me since no one here even cares. I would also like to thank Steve Ackerman, Ankur Desai, and Grant Petty for reading my thesis and giving feedback on this study.

To my officemates, thank you for letting me be my goofy weird self and putting up with my shenanigans. Thank you for reading all my emails before I hit send, letting me dance, and distract you with husky and cat videos. Thank you David Loveless for starting to peel all my clementines for me. Thank you Luke Gloege for helping me make all my plots pretty and helping me with Matlab in general. Lindsey Nytes, thank you for being my partner in climb, letting me climb my stress away, and pushing me to climb things I didn't think I could. Alex Goke, thank you for being my friend I can vent to about anything and everything, and driving to Seattle to see me give my AMS presentation. Thank you to James Simkins for introducing me to tea and having teatime nearly once a day (and sometimes twice). Speaking of tea, I appreciate all you have done for me, providing warmth on cold days, and for the caffeine to keep me awake after a late night of working.

To my friends not at UW, Wolfgang Hanft, Brooke Hagenhoff, Carlye Harris, and Garrett Layne, I am so grateful for your continued friendship. It's been so great having friends just a phone call or text away to suffer through grad school with. I'm so thankful we always try to find excuses to see each other even just for a meal passing through. Wolfgang, thank you also for making our crazy adventure dreams a reality and traveling cross-country multiple times to explore the world.

Gabe Bromley, thank you for being my favorite adventure buddy and for climbing mountains with me (literally but also the grad school mountains). Thank you for telling me on nearly a daily basis that I can do it and supporting me through the stressful times when I thought I wasn't going to finish in time.

Thank you to my wonderful family for supporting me from when I was young to follow my passion of weather. I would not be here without your love, hard work, patience, and motivation. Lastly, I would like to thank my cat, Lucy, for giving me snuggles after a long day of working.

Madison, you've given me so much these last two years; my passion for climbing, lifelong friends, and lastly, this degree. I know these will all take me far in my next chapter of life in Montana.

Table of Contents

Abstract.....	i
Acknowledgements	iii
List of Figures.....	vi
List of Tables	viii
1 Introduction.....	1
2 Background	4
2.1 Airplane Observations	4
2.2 Water Vapor Sensing System (WVSS).....	8
3 Methodology	12
4 Results	18
4.1 Surface – 400 hPa Comparisons.....	18
4.2 Ascent versus Descent Profiles	25
4.3 Radiosonde Models.....	27
4.4 Differences above Surface.....	32
4.5 700 hPa – 200 hPa Comparisons	35
4.6 Regional Comparisons	37
4.7 UPS Only Comparisons	43
4.8 Individual Locations.....	48
4.9 Individual Aircraft Comparisons.....	51
4.10 Precipitation Profiles versus Clear Profiles	55
4.11 Discussion of Differences	58
5 Conclusions.....	60
5.1 Future Work	63
References.....	64

List of Figures

Figure 2.1: The WVSS-II instrument (Image via Spectra Sensors) with a picture of how the sensor looks on an airplane (Image via NASA).....	10
Figure 2.2: Calibration run of the original WVSS-II with the chilled mirror hygrometer (Fleming and May 2004).	11
Figure 3.1: All WVSS-II observations for 2015 over the CONUS with NWS radiosonde locations plotted in black.	15
Figure 3.2: Number of aircraft soundings at each location for 2015 with locations in red being within 50 km of a radiosonde location and locations in blue being more than 50 km away from a radiosonde location.	15
Figure 4.1: WVSS-II water vapor mixing ratio value with matching radiosonde water vapor mixing ratio value plotted with color scale indicating pressure level of the match.....	20
Figure 4.2: Number of comparison profiles from the surface – 400 hPa by location for 2015.	21
Figure 4.3: CONUS composite of all comparison profiles for 2015 with the differences between the WVSS-II and the radiosondes (blue) and two standard deviations (black) (A) and the number of observations for every 10 hPa layer (B).....	22
Figure 4.4: The average of all comparison profiles by season for the CONUS. Winter (A), Spring (B), Summer (C), and Fall (D).	24
Figure 4.5: Percent differences between the WVSS-II and the Radiosondes for the seasons.25	
Figure 4.6: CONUS composite of comparison profiles split up by WVSS-II observations on ascending (blue) and descending (red) airplanes with the CONUS average (gray dashed) from Figure 4.3 A. The inset plot contains the average water vapor mixing ratio profile from the radiosondes for the CONUS.....	26
Figure 4.7: Number of observations by ascending aircraft (A) and descending aircraft (B)..	27
Figure 4.8: Comparison profiles for the CONUS split up by radiosonde type: Vaisala (A) and Lockheed Martin Sippican (B). Differences in blue and one standard deviation in black.	28
Figure 4.9: Location of the radiosondes types across the CONUS for the comparison locations in this study: Vaisala (blue) and Lockheed Martin Sippican (red).....	29

Figure 4.10: All locations 2015 average differences between the WVSS-II observations and the radiosonde type with the radiosonde type average plotted as the thicker navy line. [Lockheed Martin Sippican (A), Vaisala (B)].	30
Figure 4.11: Lockheed Martin Sippican radiosondes by season: winter (A), spring (B), summer (C), and fall (D).....	31
Figure 4.12: Vaisala radiosondes by season: winter (A), spring (B), summer (C), and fall (D).	32
Figure 4.13: Comparison profile as function of pressure above average surface pressure levels (A) and observations per layer (B).	33
Figure 4.14: CONUS composite of comparison profiles as a function of pressure above the surface comparing WVSS-II observations on during ascent (blue) and descent (red) to the CONUS average (gray dashed).....	34
Figure 4.15: 700 – 200 hPa CONUS composite of all comparison profiles with the differences between the WVSS-II and the radiosondes (blue) and two standard deviations (black) (A) and the number of observations for every 10 hPa layer (B).	36
Figure 4.16: Average WVSS-II water vapor mixing ratio profile (A), average radiosonde water vapor mixing ratio profile (B), and average radiosonde temperature profile (C). 37	
Figure 4.17: The Köppen-Geiger climate classes for the CONUS by county. (Kottek et al. 2006).	38
Figure 4.18: The regional averages from the East (blue), Mountain/Desert (red) and West (yellow) regions.	41
Figure 4.19: The fully humid East Region average with each location’s average contributing to the region and the inset showing the cities’ locations.	42
Figure 4.20: Same as Figure 4.19 but for the Mountain/Desert Region.	42
Figure 4.21: Number of comparison profiles per location for only UPS aircraft (top) and Non-UPS aircraft (bottom).	45
Figure 4.22: CONUS composite of comparison profiles using only WVSS-II observations for UPS aircraft (blue), one standard deviation for UPS aircraft (blue dashed), non-UPS aircraft (red), and one standard deviation for non-UPS aircraft (red dashed).	46
Figure 4.23: Comparisons profiles for WVSS-II observations from ascending UPS aircraft (blue), descending UPS aircraft (blue dashed), ascending non-UPS aircraft (red), and descending non-UPS aircraft (red-dashed).	47

Figure 4.24: Comparisons profiles from only UPS aircraft at 1200 UTC (blue) and 0000 UTC (blue dashed) and for Non-UPS at 1200 UTC (red) and 0000 UTC (red dashed).....	48
Figure 4.25: All comparison profiles of differences (blue) from Las Vegas, NV averaged for 2015 with two standard deviations (black) (A) and then divided by seasons: winter (B), spring (C), summer (D), and fall (E). The inset in each plot shows the average water vapor profile from the radiosondes for that time period. The black dashed line shows the average surface pressure collected from the radiosondes for the whole year.	50
Figure 4.26: Same as Figure 4.25 but for Tampa Bay, FL.	51
Figure 4.27: CONUS composite of comparison profiles using only WVSS-II observations from one aircraft with the differences between the WVSS-II and the radiosondes (blue) and two standard deviations (black) (A) and the number of observations for every 10 hPa layer (B).	52
Figure 4.28: Locations of all the comparison profiles from one aircraft.	53
Figure 4.29: Comparisons for one aircraft for ascending (blue) observations and descending (red) observations with the average (gray-dashed).	54
Figure 4.30: : Number of observations per level for one aircraft for ascending observations (A) and descending observations (B).	55
Figure 4.31: Individual cases plotted in the thinner lines with the average of the precipitating cases (blue) and clear cases (red) in the thicker lines.	57
Figure 4.32: Same as previous figure but for ascending WVSS-II observations (A) and descending observations (B).	58

List of Tables

Table 1: Locations with comparison profiles contributing to each region.	40
Table 2: List of precipitation cases and clear cases out of Atlanta/Peachtree City, GA.....	56

1 Introduction

Over the past few decades, there have been two major sources of moisture observations above the surface: radiosondes, which have a high vertical resolution and good data availability throughout the vertical column but suffer from poor spatial and temporal resolution; and satellites, which offer better spatial and temporal resolution than radiosondes but typically lack data in the lower troposphere which is crucial to understanding the development of weather events (Mati et al. 2009).

Routine airborne observations are one possible alternative that fills in the gaps of the radiosonde and satellite observing systems. Aircraft have routinely taken wind and temperature observations for their own applications, but these measurements also support forecasting by the National Weather Service by providing vertical profiles with much greater spatial and temporal density than the operational radiosonde network. Since airlines have less of a need for humidity observations than temperature and winds, moisture sensors have traditionally not been a part of this airborne dataset; however, these data are critical for accurate forecasts. Because moisture varies at smaller scales than temperature and wind, the assimilation of aircraft-based moisture data into numerical models has large positive impacts on the forecasts of the location, intensity, and timing of precipitation events (Hartung et al. 2011; Otkin et al. 2011; Petersen et al. 2016). In addition to improved weather forecasts, these additional moisture measurements could also benefit safety and efficiency in aviation, and other fields such as hydrology, atmospheric chemistry, atmospheric pollution, and global change (Fleming 1996).

Acknowledging the potential to create a complete thermodynamic profile of the atmosphere via aircraft, the Water Vapor Sensing System (WVSS) was developed to also allow for water vapor observations in addition to the temperature and wind observations already taken. After a few design alterations and testing, the current version of the WVSS-II was deployed starting in 2009 aboard over 100 mostly domestic aircraft. With the addition of water vapor measurements from the WVSS-II, four fields of information that are crucial to accurately characterize the state of the atmosphere are provided from aircraft: water vapor, temperature, wind, and pressure (Fleming and May 2004). Although inclement weather can force a reduction in flights, and thus observations, aircraft data are the only source of in situ upper-air data at asynoptic times (Moninger et al. 2003). These observations are useful by filling in spatial and temporal gaps with as many as ten high-resolution vertical profiles of the atmosphere per aircraft at different locations throughout one day (Petersen et al. 2006). A semi-accurate observation where there is no observation is useful; however, these observations are very accurate and they are measured in more places at more times than radiosondes alone making the WVSS-II observations extremely useful. Airborne observations are also cost effective with respect to the global observing system (Eyre and Reid 2014): an entire aircraft profile costs less than 5% of the cost of a complete radiosonde launch (WMO 2014b) with most of the aircraft profile costs a result of operational expenses and data management; unlike radiosondes the sensors are used over and over. Overall, when comparing a radiosonde network of ten locations to a fleet of 30 aircraft, the aircraft data program costs only 12-20% of the total radiosonde network costs over an operational period of 10 years (WMO 2014b) with many more profiles recorded.

Several studies in the past have compared the WVSS to specially launched radiosondes to validate the instrument (e.g. Fleming 2000; Moninger et al. 2003; Petersen et al. 2006; Petersen et al. 2011; Petersen et al. 2016). However, many of these studies usually only perform comparisons in a single location (e.g. Louisville, Kentucky; Rockford, Illinois) for a limited period on the order of a few weeks or months. The limited, though valuable scope of these validation studies prevents the examination of seasonality in the instrument and its performance in different climate regimes. The present work extends these validation studies to investigate how the WVSS-II performs relative to the operational National Weather Service (NWS) radiosonde network for an entire year. By examining how the WVSS-II behaves throughout the entire United States for an annual cycle instead of a time limited study at one location, it is possible to assess how the accuracy of the WVSS-II varies in different seasons and water vapor environments. As the data have already been found to improve forecasting skill at the fraction of the cost of radiosondes and there are plans to also begin using the data with climate study applications (WMO 2014b; Rahn and Mitchell 2016), it is imperative to fully characterize the accuracy of the WVSS-II system. Examining the geographical and seasonal variations in accuracy allows for an increase in confidence in this instrument and also enables for correction schemes to be implemented for any observed differences.

2 Background

2.1 Airplane Observations

The first airborne meteorological observation took place in 1912 in Germany when a meteorograph was installed on an Euler monoplane and used to record temperature and pressure at altitudes up to 1100 m (Wendisch and Brenguier 2013). In the United States, the collection of meteorological data from aircraft began in 1919 when the United States Weather Bureau began paying pilots to fly with “aerometeorographs” attached to their aircraft (Hughes and Gedzelman 1995; Moninger et al. 2003). By 1937, the United States government had funded 30 soundings per day to be collected by civilian and military aircraft. Pilots would not get paid unless they reached 13,500 ft and for every additional 1,000 ft, they were given a 10% bonus; however, twelve pilots were killed between 1931 and 1939 due to blacking out from a lack of oxygen at those high altitudes (Hughes and Gedzelman 1995; Moninger et al. 2003). The development of the radiosonde in the early 1930s promised a simpler and safer method of obtaining atmospheric profiles and by 1940, operational thermodynamic soundings were entirely performed by radiosondes (Moninger et al. 2003), though aircraft observations continued to be used for turbulence and occasional scientific studies (Wendisch and Brenguier 2013).

The First Global Atmospheric Research Program (GARP) Global Experiment (FGGE), a study designed to gather routine and experimental data using a number of observing systems to improve and validate theoretical models of the atmosphere’s behavior, engendered a reevaluation of the potential for operational airborne instrumentation. Commercial aircraft equipped with meteorological instruments were one of the many observing systems that were part of this project. These aircraft recorded wind and temperature measurements using two

different types of recording systems: the Aircraft Integrated Data Systems which recorded the data to cassettes which were processed after the aircraft landed and the Aircraft to Satellite Data Relay (ASDAR), which allowed the data to be transmitted in real-time via geostationary satellites. The ASDAR-equipped aircraft were found to be useful by providing information in data-sparse regions and continued to provide measurements for up to 20 years beyond the conclusion of GARP in 1982 (Sparkman et al. 1981; Fein et al. 1983; Petersen 2016). The proliferation of aircraft observations continued to increase substantially through the 1990s (Sparkman et al. 1981; Giraytys et al. 1981; Lord et al. 1984; Fleming 1996; Moninger et al. 2003). These projects showed the benefits of the high-quality wind and temperature observations especially in regions that influence the predictions of cyclogenesis and storm evolution (such as the high kinetic energy region around the jet stream) (Petersen 2016). The original system within the United States to collect the automated commercial aircraft reports was known as the Meteorological Data Collection and Reporting System (MDCRS; Martin et al. 1993). Eventually, this system became a part of the World Meteorological Organization's (WMO) Aircraft Meteorological Data Relay (AMDAR) program (WMO 2003, 2014a). Currently, 680,000 observations of wind and temperature are collected daily by 3,500 aircraft from 39 airlines globally. More than 100 of these aircraft, mainly the United States, also provide moisture data (Petersen 2016).

Since the data collected from aircraft naturally follow the ebb and flow of commercial air traffic, observations are highly variable in time with evening peaks and early morning minima (Jamison and Moninger 2002; Moninger et al. 2003). The number of reports also decrease on weekends due to reduced flights from cargo operators like FedEx and UPS (Moninger et al. 2003). Most of the data below 7600 m (25,000 ft) is concentrated near

major hubs and essentially provides a sounding of the atmosphere when aircraft take off or land (Jamison and Moninger 2002; Moninger et al. 2003). The observations also vary when certain weather conditions are present; unlike many meteorological observing systems, inclement weather forces a reduction in observations since flights are frequently canceled, with the greatest disruption caused by ice and snow. For example, a January 2002 blizzard on the East Coast of the United States had far-reaching impacts across the nation, even causing an 8% decrease in the number of aircraft profiles as far away as Denver since the cancelled flights were not departing their airports of origin (Moninger et al. 2003).

Prior studies have compared aircraft-based observations of temperature and wind data with radiosondes to quantify the magnitude of measurement bias (e.g. Schwartz and Benjamin 1995; Moninger et al. 2003). Schwartz and Benjamin (1995) compared the aircraft observations to NWS-operated radiosondes launched with a 3 h frequency in Denver, CO. They found that differences between the radiosondes and aircraft data were equal to previous estimates of radiosonde errors alone indicating higher accuracy of temperature and wind observations than from radiosondes. However, in similar studies, it has been found that a slight warm bias at all levels is present that increased above 500 hPa which could be due to the spatial differences between the radiosonde and the aircraft (Mamrosh et al. 2006; Ballish and Kumar 2008; Zhu et al. 2015). Overall, it has been accepted that aircraft winds, which are obtained via the internal navigation system of the plane, are more accurate than the radiosonde winds (Fleming 1996).

National Weather Service (NWS) Weather Forecast Offices (WFOs) have found many operational uses for WVSS-II operations; these uses can be seen by examining NWS forecast discussions. Some examples of their use include assisting in forecasting the initiation time of

severe thunderstorms (Moninger et al. 2003), locating wind and temperature gradients (Petersen 2016), and providing profiles of the atmosphere where radiosondes are absent temporally and spatially (Petersen et al. 2016). The data provided by aircraft are also important to the aviation community by improving safety and fuel efficiency, as in situ wind observations can aid in planning efficient flight routes (Fleming 1996).

While forecasters clearly benefit by having these real time observations throughout the depth of the atmosphere at high temporal resolution, numerical weather prediction (NWP) models also benefit from airborne observations since these data provide information about the state of the atmosphere that would otherwise go unobserved. The assimilation of WVSS-II observations into NWP has been shown to improve forecast skill (DiMego et al. 1992; Bell 1994; Schwartz and Benjamin 1995; Petersen 2016). In fact, aircraft data are the largest non-satellite contributor to data assimilation systems (Isaksen 2014). The data have the highest impact per cost for forecast sensitivity to observations when compared with other observing systems on shorter forecast time scales during periods where aircraft data density is greatest, such as during the daytime and early evenings (Eyre and Reid 2014; Petersen 2016). These observations continue to increase regional and global scale forecasts for even medium-ranges (Langland and Baker 2004) and contribute 10-15% to the 24 hour forecast skill improvement (Petersen 2016). At the European Centre for Medium-Range Weather Forecasts (ECMWF), to correct for the biases that have been found, a correction scheme designed by Isaksen et al. (2012) has been implemented with other centers having plans for similar schemes to be implemented in the future. This scheme has been found to improve the upper-level temperature analyses and near tropopause satellite measurement agreements. (Zhu et al. 2015).

2.2 Water Vapor Sensing System (WVSS)

The Water Vapor Sensing System (WVSS) is an aircraft-mounted calibrated sensor that measures water vapor content. The first WVSS measured relative humidity using a thin-film capacitive sensor similar to those found on radiosondes (Petersen and Moninger 2006; Petersen et al. 2006; Mamrosh et al. 2006). An initial deployment in 1999 involving the first version of the WVSS aboard six United Parcel Service (UPS) aircraft was validated during a short experiment in which radiosondes were launched near UPS's Louisville, Kentucky hub coincident with arriving and departing aircraft; the data were comparable to radiosonde observations of moisture (Mamrosh et al. 2006). In 2001, this study was expanded to include 16 WVSS-equipped aircraft and a several month validation period. These studies determined that the sensor had excessive relative humidity biases that were unacceptable and it did not respond quickly enough to rapid changes in moisture (Petersen et al. 2006; Petersen et al. 2016). In addition, the sensor required maintenance with a frequency that the airlines found burdensome (Fleming 2002; Mamrosh et al. 2006).

Because of the issues with the first version of the WVSS, a completely different sensor that consisted of a laser diode was designed and designated as WVSS-II. The diode operates at a single wavelength of 1.37 μm which allows the sensor to directly count the number of water vapor molecules moving past the sensor in a specific volume of air, thus providing a direct measurement of water vapor mixing ratio and allowing the moisture observations to be independent of the temperature and wind observations made by the aircraft (Fleming and May 2004; Petersen et al 2016).

Versions one and two of the WVSS-II were deployed beginning in 2005. Again, aircraft to radiosonde comparisons were made to determine the accuracy of the WVSS-II

(Petersen et al. 2006). Problems with these versions were found that included encoding precision issues that led to an increase in biases above 10 g kg^{-1} because of a precision of only 1 g kg^{-1} , problems with the internal laser seals leading to water vapor contamination producing moist biases, and large biases and other errors produced by temperature-sensitive components of the sensor (Helms et al. 2010; Petersen et al. 2016).

Version three of the WVSS-II (Fig. 2.1) corrected these problems and began to be deployment in 2009 (Hoff 2009; Helms et al. 2010). Currently, the sensor is aboard Southwest and UPS 757s and 737s. Like the previous versions, version three uses the standard aircraft 28-volt power supply and only has a small protuberance on the exterior of the aircraft. The new version weighs 3.5 kg, slightly heavier than the previous versions (Fleming and May 2004; Spectra Sensors 2012). It has a range of detectable signal of 50 ppmv to 40,000 ppmv with an accuracy of $\pm 50 \text{ ppmv}$ or $\pm 5\%$ of the reading (whichever is greater). The operating temperature range for the WVSS-II is $-65 \text{ }^{\circ}\text{C}$ to $+50 \text{ }^{\circ}\text{C}$ while the sampling pressure ranges from the surface (1016 hPa) to 200 hPa (Spectra Sensors 2012). It samples four times per second and can output a measurement every 2.3 seconds (Spectra Sensors 2012, Petersen et al. 2016). Typically, descending aircraft record a WVSS-II observation about once every 1,000 ft whereas ascending aircraft record an observation about once every 300 ft. For ascending aircraft below 650 hPa, the frequency in which the WVSS-II is recording measurements is at a much higher frequency than above 650 hPa. In addition, aircraft are often instructed to temporarily level off at 10,000 ft (approximately 700 hPa) above mean sea level before continuing the ascent or descent. The cargo carriers format the data to provide the highest vertical resolution at low-levels (Jamison and Moninger 2002; Moninger et al. 2003). The high frequency of sampling for the WVSS-II allows for vertical

moisture profiles to be collected at a similar frequency of a radiosonde (Petersen et al. 2016). Hoff (2009) performed chamber tests of this newest version of the sensor at the German Weather Service (known by its German acronym DWD) and found the detection limit to be lower than the previous versions with the sensor still reacting well at an extremely low water vapor value of 0.02 g kg^{-1} (Helms et al. 2010). This lower detection limit allows detection of water vapor in the upper troposphere and lower stratosphere, around 400 hPa in winter to 200 hPa in the summer (Hoff 2009; Helms et al. 2010; Petersen et al. 2016). The DWD tests also showed a small dry bias of 5-7% from $1 - 10 \text{ g kg}^{-1}$ and most readings were within $\pm 10\%$ below 0.5 g kg^{-1} (Hoff 2009; Helms et al. 2010).

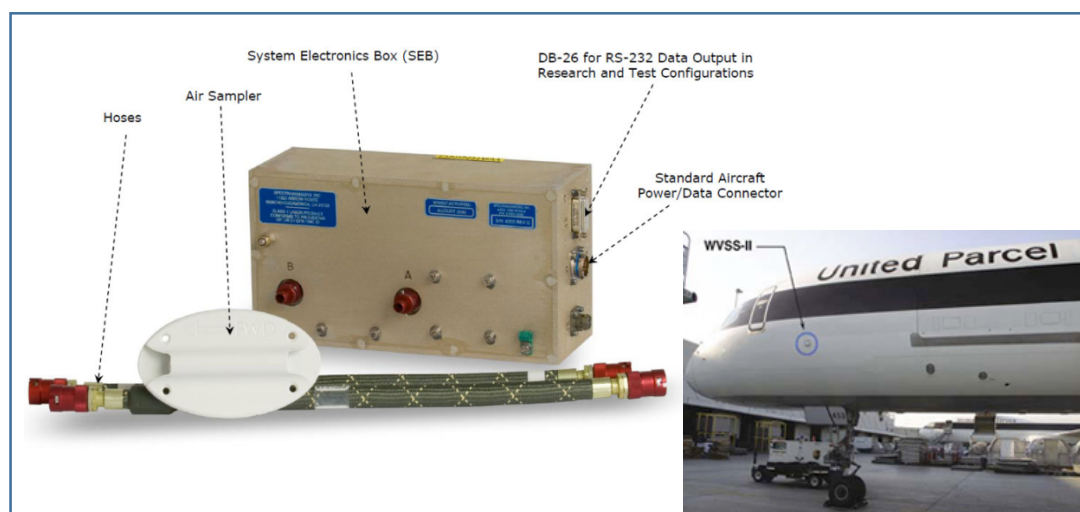


Figure 2.1: The WVSS-II instrument (Image via Spectra Sensors) with a picture of how the sensor looks on an airplane (Image via NASA).

Calibration and test runs of the WVSS-II have been performed through all versions of the sensors. Figure 2.2 shows how the original WVSS-II performed in comparison to a chilled mirror. Fleming and May (2004) comment positively on how fast the WVSS-II recovers in comparison to the chilled mirror, while Helm et al. (2010) discuss how the differences in the output from the chilled mirror and the WVSS-II could be explained

possibly by the much faster response time of the WVSS-II compared to the chilled mirror.

The improved reliability demonstrated by these tests coupled with the reduced maintenance requirements of the latest version enabled WVSS-II to gain acceptance by major airlines for deployment aboard their fleet.

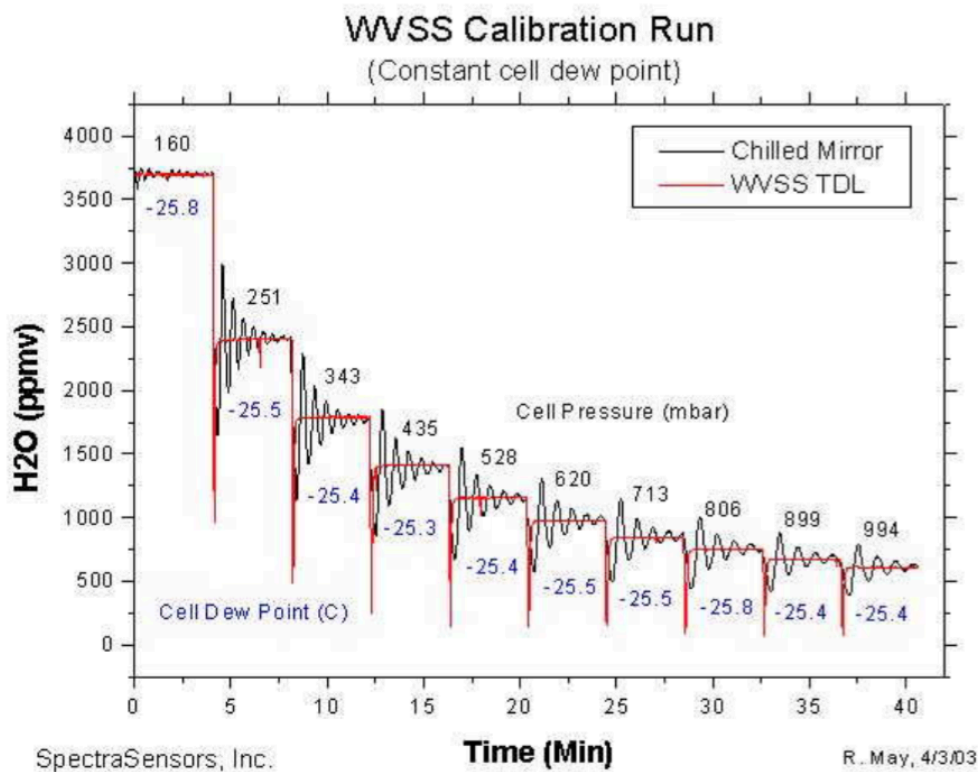


Figure 2.2: Calibration run of the original WVSS-II with the chilled mirror hygrometer (Fleming and May 2004).

3 Methodology

The WVSS-II data are provided within Aircraft Meteorological Data Reports (AMDAR) that are transmitted to the ground via the Aircraft Communications Addressing and Reporting System (ACARS) (ESRL/GSD). AMDAR reports contain the water vapor information from the WVSS-II along with all other meteorological data collected from commercial aircraft such as temperature and winds and their corresponding altitudes and locations.

Operational NWS radiosondes were compared with the WVSS-II data and were considered “truth” for this study; the focus on operational radiosondes results in a much larger spatial and temporal extent for the present validation study as compared to previous validation studies. It is important to note that comparing the WVSS-II to radiosondes does not assume that the radiosondes are better than the WVSS-II. This is done because the radiosondes are the only moisture observations available at high vertical resolution for comparisons to be made.

The NWS currently uses two different radiosonde models: the LMS-6 by Lockheed Martin Sippican and the RS92-SGP by Vaisala (NOAA 2016). Regardless of the model, the radiosonde data include pressure, temperature, relative humidity, latitude and longitude of the observations, and altitude. These radiosondes allow for tracking of the balloon via the GPS coordinates, allowing better comparisons with airplane locations since previous studies have assumed the radiosonde location to be at the location of launch throughout the profile (e.g. Mamrosh et al. 2006). The LMS-6 uses a thin film capacitance relative humidity sensor with a range of 0 – 100% and an accuracy of +/- 5% and a pressure range of 1080 hPa to 3 hPa with an accuracy of better than 0.5 hPa (Gov tribe website – need to find better reference). The RS92-NGP radiosonde uses a thin-film capacitor as well for the humidity sensor with a

range of 0 – 100% and an accuracy of 5%. The pressure range is from 1080 hPa to 3 hPa with an accuracy of 1 hPa from 1080 hPa to 100 hPa (Vaisala 2015). Since dew point temperature is the unit of record for radiosonde humidity observations, the relative humidity data for both sensors are converted to dew point temperatures during post-processing. As the WVSS-II directly measures water vapor mixing ratio by counting molecules, the radiosondes were converted from dew point temperatures to water vapor mixing ratio by first calculating the vapor pressure using eq. (1) then calculating mixing ratio from the vapor pressure using eq. (2)

$$e = 6.112 * \exp\left(\frac{17.67 * T_d}{T_d + 243.5}\right) \quad \text{eq. (1)}$$

$$w = 0.622 * \frac{e}{P - e} \quad \text{eq. (2)}$$

where P is the pressure from the radiosonde in pascals and T_d is the dew point temperature in degrees Celsius (Petty 2008). This conversion from dew point temperature to water vapor mixing ratio allows for a more direct comparison between the water vapor values of the WVSS-II and the radiosondes. If the WVSS-II were to be converted to relative humidity or dew point using the temperature from the aircraft, there could be a bias in the relative humidity value due to possible biases within the aircraft temperature measurements (Mamrosh et al. 2006 Helms et al. 2010; Petersen et al. 2006).

The coverage of the water vapor reports for 2015 with NWS radiosonde locations across the continental United States (CONUS) is shown in Figure 3.1. The color scale of Figure 3.2 is the base 10 logarithm of the number of observations per day for 0.25 degree by 0.25 degree boxes; a value of one on the map indicates ten observations per day at that location. This map allows for identification of possible locations for comparison and also shows where

AMDAR data could potentially fill in gaps in the radiosonde network and allow for an increase in the number of tropospheric soundings. Large cities such as Chicago, IL; Dallas, TX; and Denver, CO are easily identifiable with large numbers of airplanes taking off and landing at their airports. By contrast, population sparse regions, such as in the northern parts of the CONUS, have very few WVSS-II observations. In some of these locations, the only WVSS-II observations are from planes flying over a radiosonde site at upper altitudes but not taking off or landing nearby. This is also shown in figure 3.2 which shows the number of aircraft profiles per airport for 2015. Locations in blue are airports that are greater than 50 km away from a radiosonde location show areas where vertical profiles of the atmosphere now exist from aircraft data. Locations in red are within 50 km of a radiosonde location show the idea locations for comparisons of radiosondes and aircraft data. These locations such as Dallas, Texas; Denver, Colorado; and Atlanta, Georgia; were identified to be used for comparison between the WVSS-II and NWS radiosondes. Comparisons between the WVSS-II and NWS radiosondes were completed for all of 2015 for both types of radiosonde across the CONUS, at individual locations, for aircraft ascending/descending into an airport, over different climate regions determined by the Köppen-Geiger climate class, for UPS and non-UPS aircraft, and for one individual aircraft.

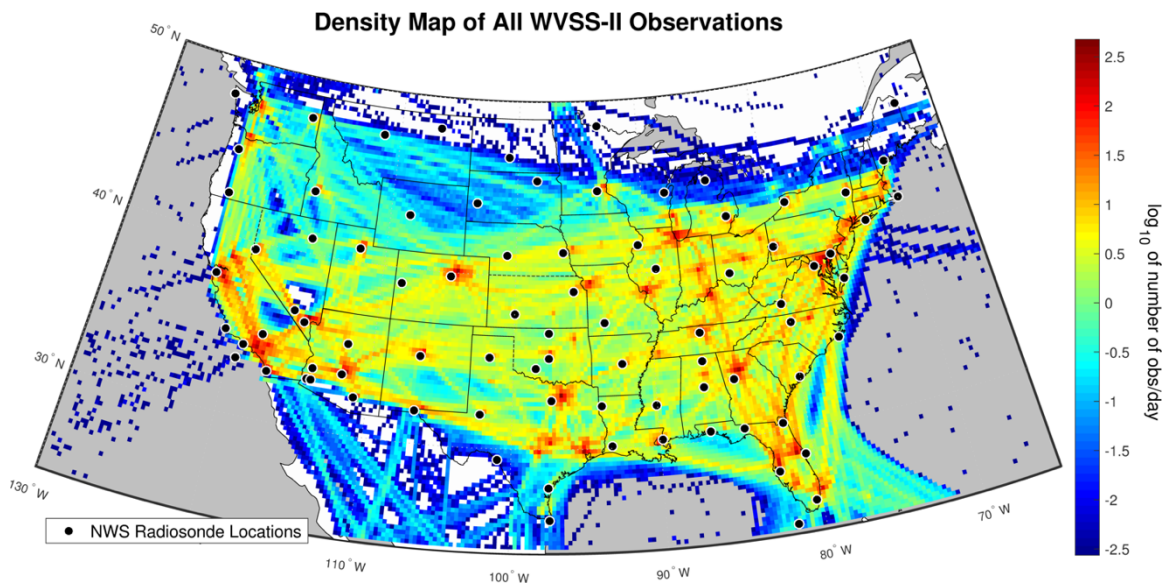


Figure 3.1: All WVSS-II observations for 2015 over the CONUS with NWS radiosonde locations plotted in black.

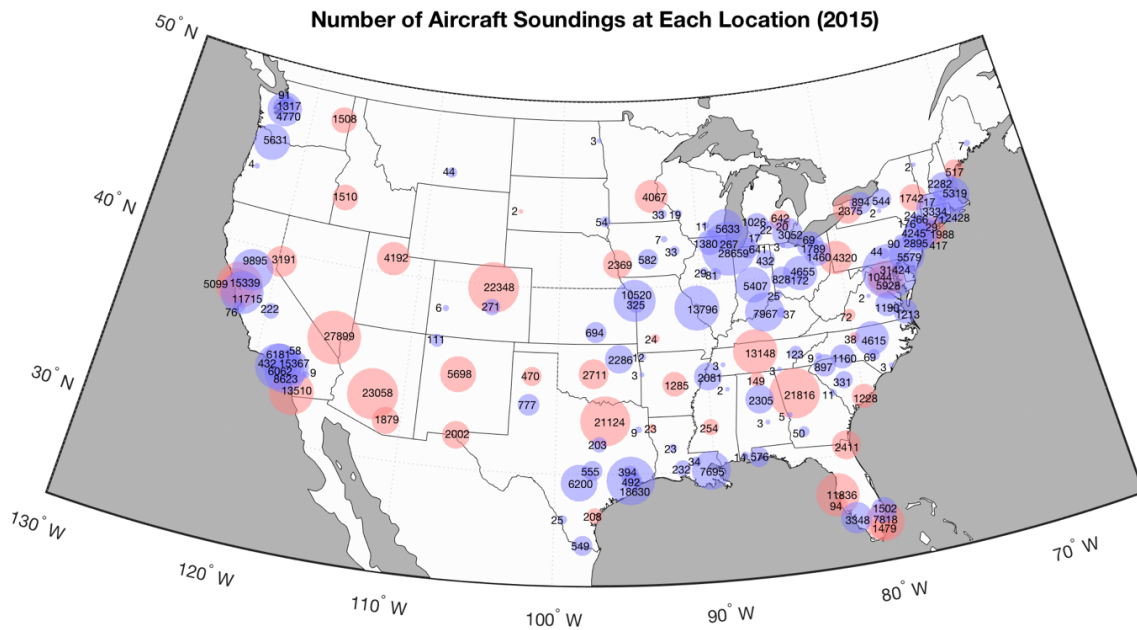


Figure 3.2: Number of aircraft soundings at each location for 2015 with locations in red being within 50 km of a radiosonde location and locations in blue being more than 50 km away from a radiosonde location.

To compare the WVSS-II data to NWS radiosondes, the following criteria were implemented, consistent with previous validation studies (e.g. Petersen et al. 2006; Petersen et al. 2016):

- The airplane observation must contain a WVSS-II water vapor observation.
- The airplane observation must be within +/- 30 min of the radiosonde observation.
- The airplane observation must be within +/- 10 hPa of the radiosonde observation.
- The airplane observation must be within a 50 km radius of the radiosonde observation.
- For low-level comparisons only, the airplane observation must come from or be landing at an airport near the radiosonde launch location.

These criteria allow for both the airborne observation and the radiosonde comparison to be spatially and temporally similar in order to create the most accurate comparisons possible. For low-level comparisons (below 400 hPa or about 7200 m), the airplane must be landing or taking off from an airport near the radiosonde launch location to ensure the airplane is either ascending or descending and therefore creating a profile for comparison instead of merely flying over the comparison location while headed to some other destination. The points remaining from the airplane, along with the radiosonde profile, were then interpolated onto the same vertical 10 hPa grid from 1050 hPa to 400 hPa for each radiosonde. Differences between the airplane and the radiosonde were calculated by subtracting the calculated radiosonde water vapor value from the WVSS-II water vapor value. A positive difference informs of the WVSS-II is moister than the radiosonde and a negative value informs the WVSS-II is more dry.

Higher level comparisons were also completed from 700 hPa to 200 hPa. These higher level comparisons use the same locations as the lower-level comparisons and follow all the same criteria for the low-level comparisons except for the airport restraint. This allows for planes higher in altitude to be included and indicates how the WVSS-II performs at cruising altitudes as well. The overlap between the lower level and the upper level comparisons enables the examination of how the mid-levels differ with and without the airport restraint.

4 Results

4.1 Surface – 400 hPa Comparisons

Comparisons made for the pressure range from the surface to 400 hPa required WVSS-II measurements to be aboard an airplane that was taking off or landing from an airport near the comparison radiosonde location. Figure 4.1 shows the WVSS-II water vapor mixing ratio values plotted with the corresponding radiosonde water vapor mixing ratio value with the color scale showing the pressure level in which the match up was made. In general, the match-ups follow the one-to-one comparison line. However, there are a few cases where outliers are present. These cases tend to show a constant WVSS-II value for an entire take-off or landing of an aircraft since it is seen how the constant values change with pressure. This could be caused by a faulty sensor on one aircraft or a sensor with an amount of moisture trapped in the air sampler.

When doing a t-test for the paired matches, the means for the radiosonde water vapor mixing ratio and the WVSS-II water vapor mixing ratio are different when viewing the atmosphere at approximately the same place and time. These would be expected to be different though because the quality of the moisture sensor on the radiosondes is far less than the laser diode of the WVSS-II. In addition, when converting the relative humidity of the radiosonde to water vapor mixing ratio temperature is used. For the radiosondes, there are known temperature biases that would be effecting the moisture measurements causing the difference.

Figure 4.2 locates where comparisons were found. The number at each location represents the number of comparison profiles made. In general, the number of comparison profiles is higher in the east and decreases westward. This is because operational

radiosondes are launched at 1100 UTC and 2300 UTC to be valid for the synoptic observation hours of 1200 UTC and 0000 UTC. In the Eastern Time zone, the 1100 UTC launch times are at 7:00 AM local time during daylight savings time (6:00 AM during standard time), a time when many flights are operating. However, in the Pacific Time zone, this launch time corresponds with 3:00 AM or 4:00 AM depending on the time of the year, an unpopular time for passenger flights. This is not as significant an issue for the 0000 UTC radiosondes, which occur at popular times for flights on either coast. Locations like Atlanta, Georgia have nearly two comparison profiles per day while Denver, Colorado and Oakland, California have about one comparison profile per day. Other locations such as Amarillo, Texas and Pittsburg, Pennsylvania have less than one comparison profile per week, made when a WVSS-II equipped airplane just happened to visit an airport coincident with a radiosonde launch.

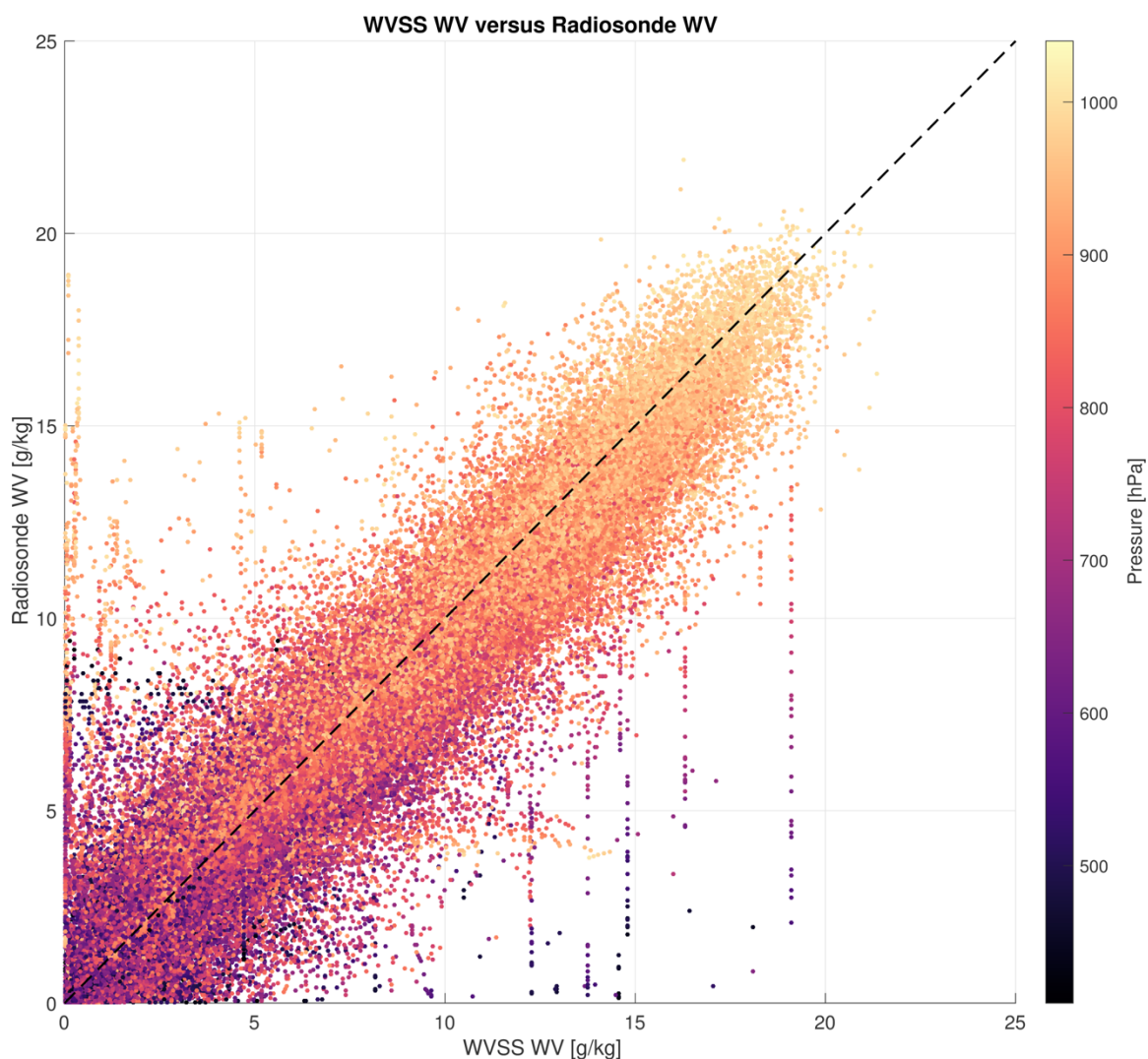


Figure 4.1: WVSS-II water vapor mixing ratio value with matching radiosonde water vapor mixing ratio value plotted with color scale indicating pressure level of the match.

Figure 4.3 is the average of all of these comparisons profiles from across CONUS. Above 1000 hPa, the WVSS-II is slightly moister than the radiosondes through 400 hPa which follows what Petersen et al. (2016) found as well. Below 1000 hPa, the WVSS-II is slightly dry (Fig. 4.3 A). This dry differences coincides with a drastic decrease in the number of observations per layer (Fig. 4.3 B). This decrease in observations could be due to the fact that places at higher elevations (e.g. Denver, Colorado, elevation 1655 m) never have

pressure readings this high meaning only a few comparison locations would be contributing to average at these levels. Also found on Figure 4.3 A is the RMS value found from Petersen et al. 2016. This value is 0.8 g kg^{-1} for WVSS-II observations compared with radiosondes with 50 km, 10 hPa, and 30 minutes. When Petersen et al. (2016) compared WVSS-II observations within 60 km of each other within 15-30 minutes, the value was less than 0.4 g kg^{-1} . They suggested that errors in the radiosonde moisture measurements were causing a greater contribution to the observed differences than any WVSS-II errors.

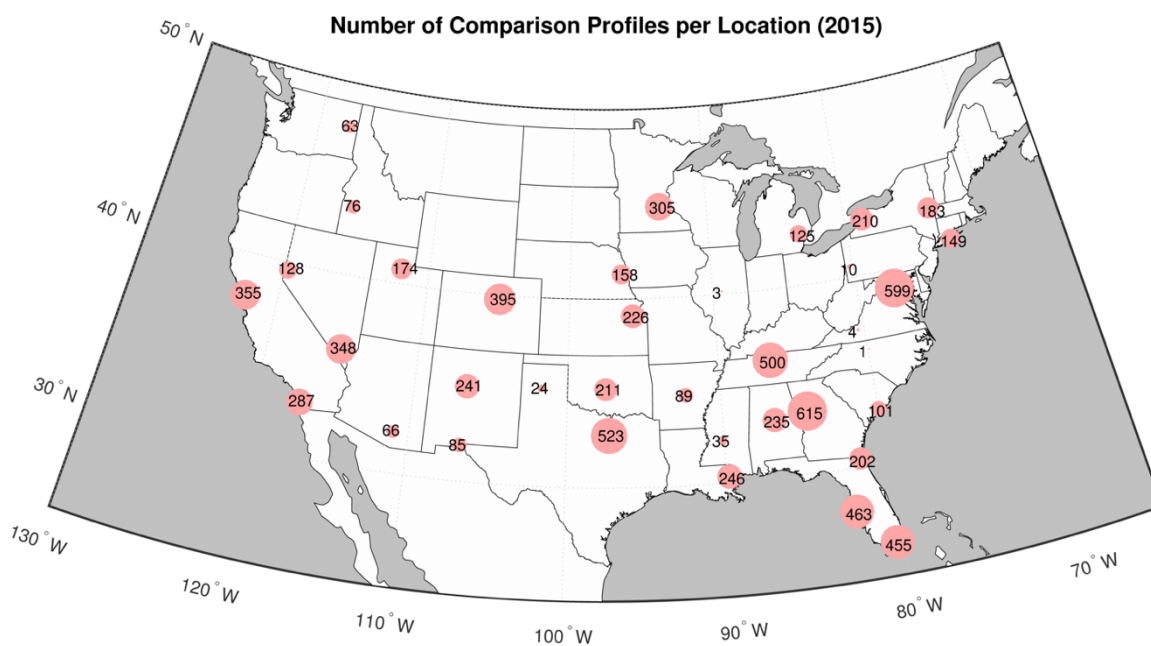


Figure 4.2: Number of comparison profiles from the surface – 400 hPa by location for 2015.

The number of observations per level (Fig. 4.3 B) shows a maximum in observations at approximately 940 hPa decreasing steadily with height until a second maximum occurs at 680 hPa where it once again decreases with altitude. This second maximum occurs due to the frequency in which observations are made by the WVSS-II and the flight patterns of

aircraft. Below 650 hPa, the frequency in which the WVSS-II is making measurements is at a much higher frequency for ascending aircraft than above 650 hPa while the typical aircraft rate of ascent decreases at around 700 hPa. This decrease in ascent rate combined with a higher level of sampling increases the number of observations from approximately 700 – 650 hPa.

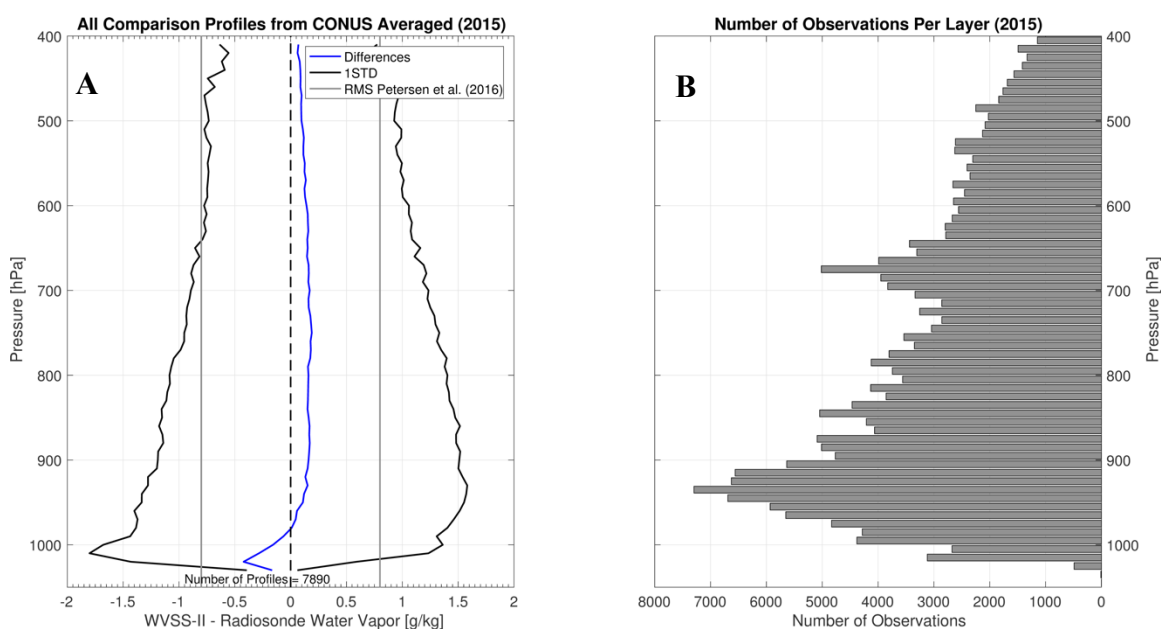


Figure 4.3: CONUS composite of all comparison profiles for 2015 with the differences between the WVSS-II and the radiosondes (blue) and two standard deviations (black) (A) and the number of observations for every 10 hPa layer (B).

One of the advantages of doing a study with a year-long body of data is the ability to examine the performance of WVSS-II in different seasons. As can be seen in (Fig. 4.4), individual seasons have a dramatically different difference profile than the year as a whole. Winter has the smallest differences with larger differences in spring. The maximum of differences occurs during the summer with the WVSS-II being much moister than the

radiosondes. Fall then has a decrease in differences. However, the amount of water vapor present in the atmosphere at these different times of year vary. Examining the differences by percent differences shows that throughout the seasons the percent difference between the WVSS-II and the radiosondes (Fig. 5) are nearly of the same magnitudes. The percent differences would be expected to increase with height since the water vapor values are so small in magnitude. At the lowest levels, spring is the only season where the minimum in percent difference is not at the surface. Overall though, it displays the sensor does not change in performance throughout the seasons.

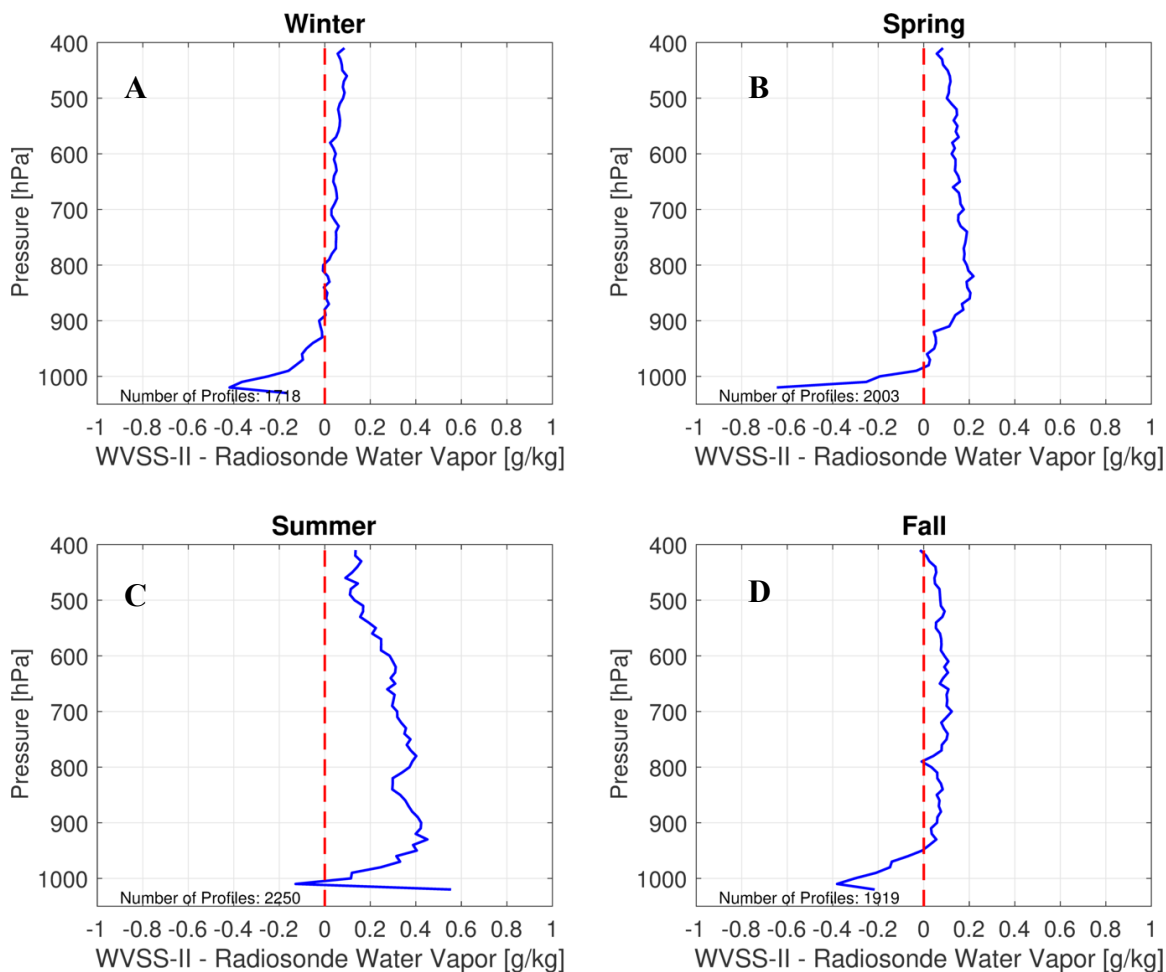


Figure 4.4: The average of all comparison profiles by season for the CONUS. Winter (A), Spring (B), Summer (C), and Fall (D).

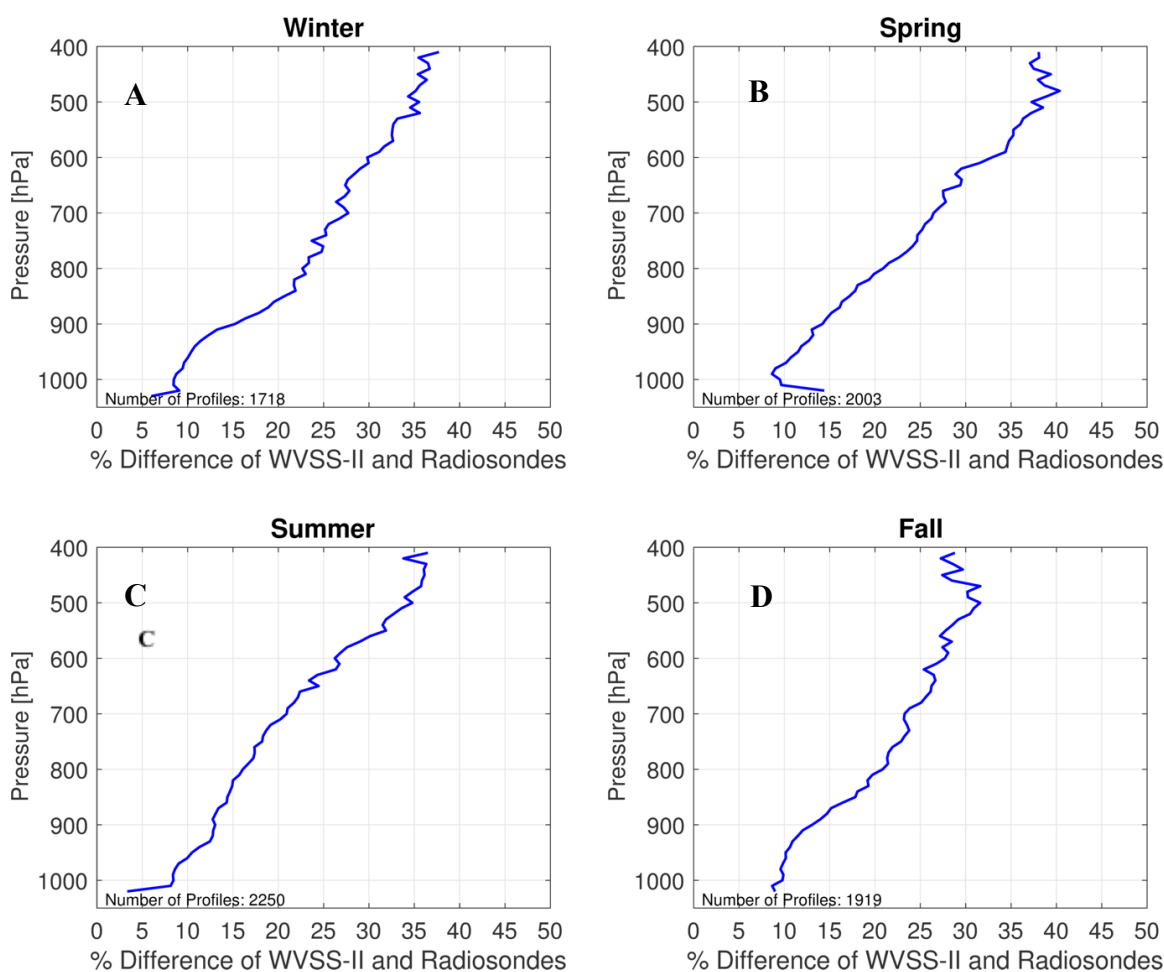


Figure 4.5: Percent differences between the WVSS-II and the Radiosondes for the seasons.

4.2 Ascent versus Descent Profiles

Previous studies (Petersen et al. 2011, Petersen et al. 2016) have found differences between the ascending and descending observations from the WVSS-II, a finding replicated here across the CONUS. This can be seen in Figure 4.6. The ascent and descent profiles have similar structures [also found in Petersen et al. (2011)], but it is apparent that the WVSS-II observations from ascending airplanes are slightly moister than radiosondes when compared to the CONUS composite while the descending observations are slightly drier than the CONUS composite from about 950 hPa – 600 hPa. The smaller difference found in the

descending data was also found by Petersen et al. (2016). The possible hysteresis could be explained by the fact as an aircraft ascends it typically moves from moister levels to more dry ones, but moist air may remain in the sensor. The opposite is true for descending aircraft.

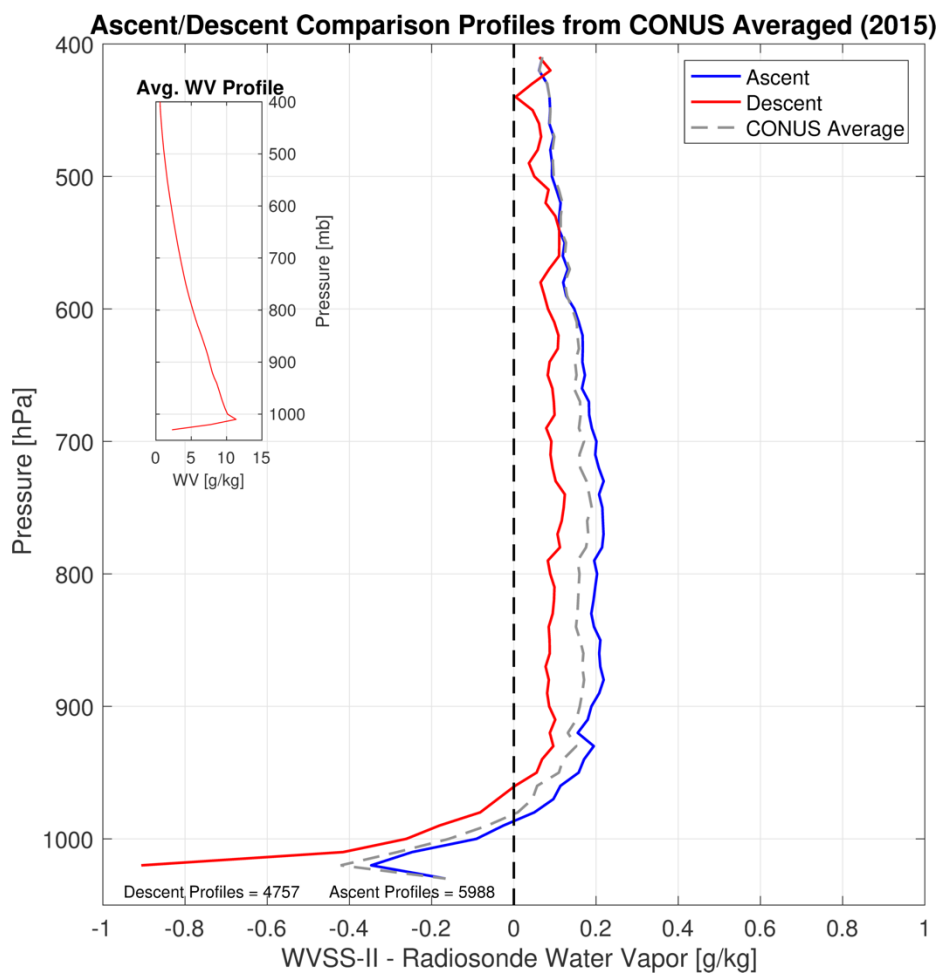


Figure 4.6: CONUS composite of comparison profiles split up by WVSS-II observations on ascending (blue) and descending (red) airplanes with the CONUS average (gray dashed) from Figure 4.3 A. The inset plot contains the average water vapor mixing ratio profile from the radiosondes for the CONUS.

The number of observations per layer for ascending and descending planes (Fig. 4.7) show that the number of WVSS-II observations on descending aircraft is about one-third of

the number of observations on ascending aircraft. This is an additional result of the frequency the observations are recorded for ascending and descending aircraft. Descending aircraft record a WVSS-II observation about once every 1,000 ft whereas ascending aircraft record a WVSS-II observation about once every 300 ft. This difference in recording frequency explains the differences in the number of observations per layer for the ascending and descending aircraft.

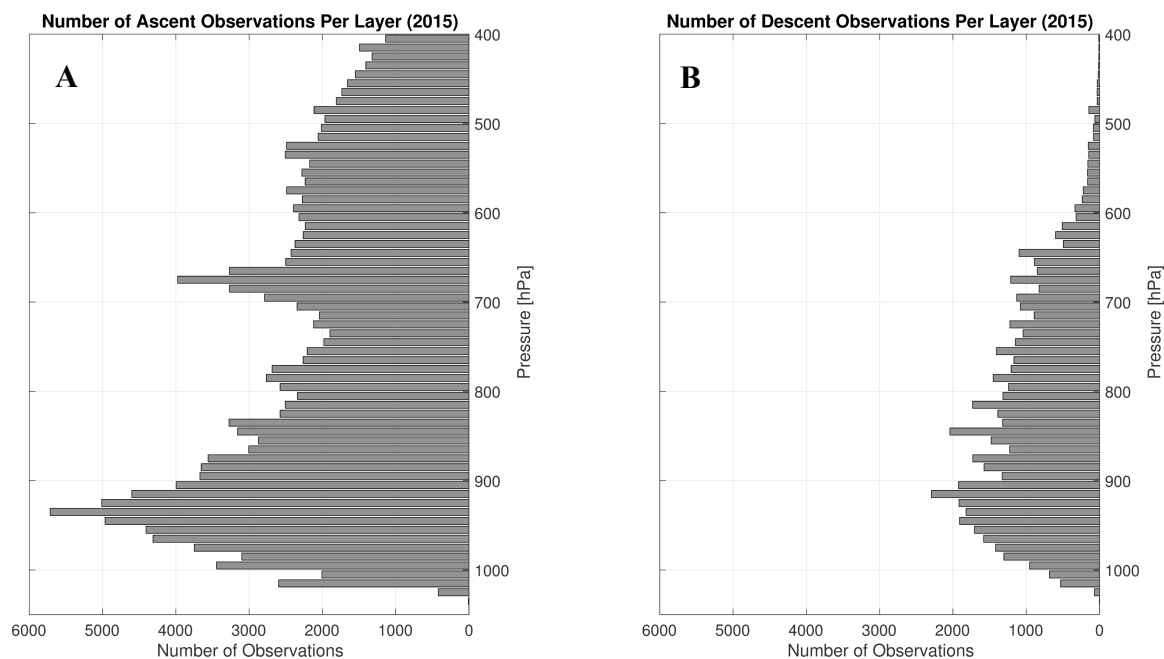


Figure 4.7: Number of observations by ascending aircraft (A) and descending aircraft (B).

4.3 Radiosonde Models

NWS operates two different types of radiosondes and each has its own set of biases, so comparisons between WVSS-II and radiosonde must be performed by radiosonde type (Fig. 4.8). The Vaisala RS92-SGP radiosonde has been found to have a radiation dry bias most likely due to solar heating of the sensor which is a function of pressure and therefore

more impactful in tropical regions where the tropopause is higher (Vömel et al. 2007). However, a correction scheme has been implemented in post-processing to correct for this bias (Wang et al. 2013). The biases do not appear to be as strong for the Lockheed Martin Sippican LMS6 and no correction schemes have been developed for them. Figure 4.8 A shows the Vaisala RS92-SGP while Figure 4.8 B shows the Lockheed Martin Sippican LMS6. For both radiosonde models, the WVSS-II observations are slightly drier at the surface than the radiosondes but the Vaisala dry difference continues to nearly 800 hPa while the LMS is only to about 1000 hPa. The LMS comparisons echo the CONUS composite; this is most likely due to the fact that the LMS makes up about 80% of the radiosondes used in this study.

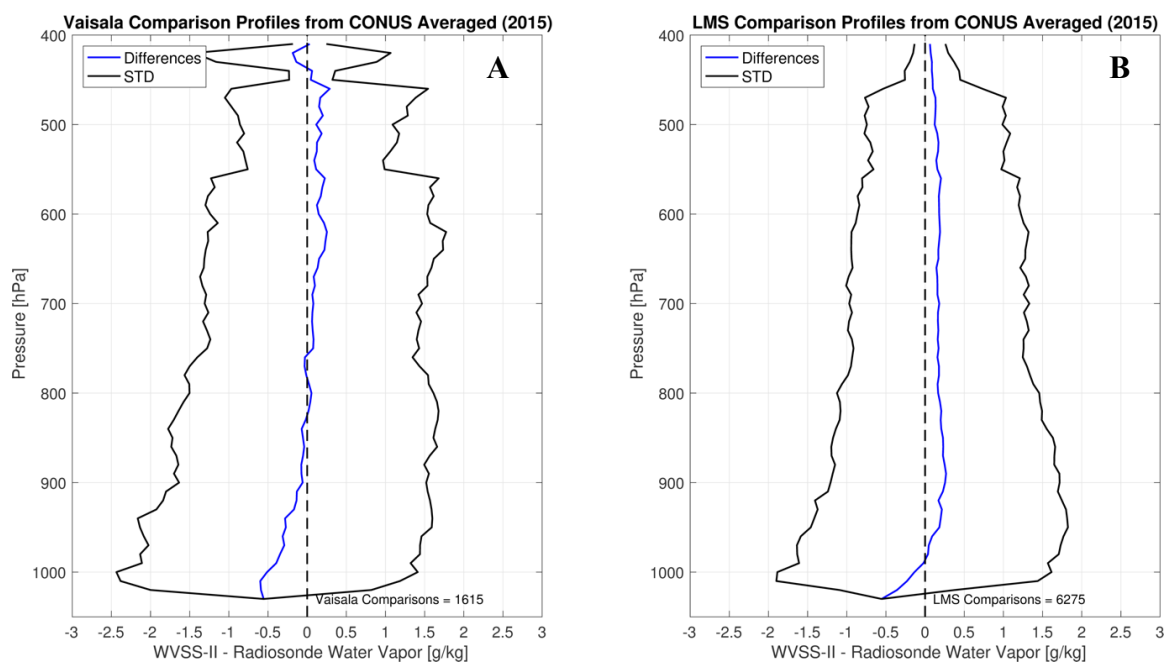


Figure 4.8: Comparison profiles for the CONUS split up by radiosonde type: Vaisala (A) and Lockheed Martin Sippican (B). Differences in blue and one standard deviation in black.

To further examine the differences between the radiosonde types, it is crucial to know where the different radiosondes are being launched (Fig. 4.9). The Vaisala radiosonde locations are distributed across the CONUS with five of the eight locations being along the coast. With more than half of the Vaisala radiosondes being launched at coastal locations, the predominately maritime environments of the Vaisala radiosondes could be introducing a bias that is not controlled for in this set of comparisons to the LMS radiosondes.

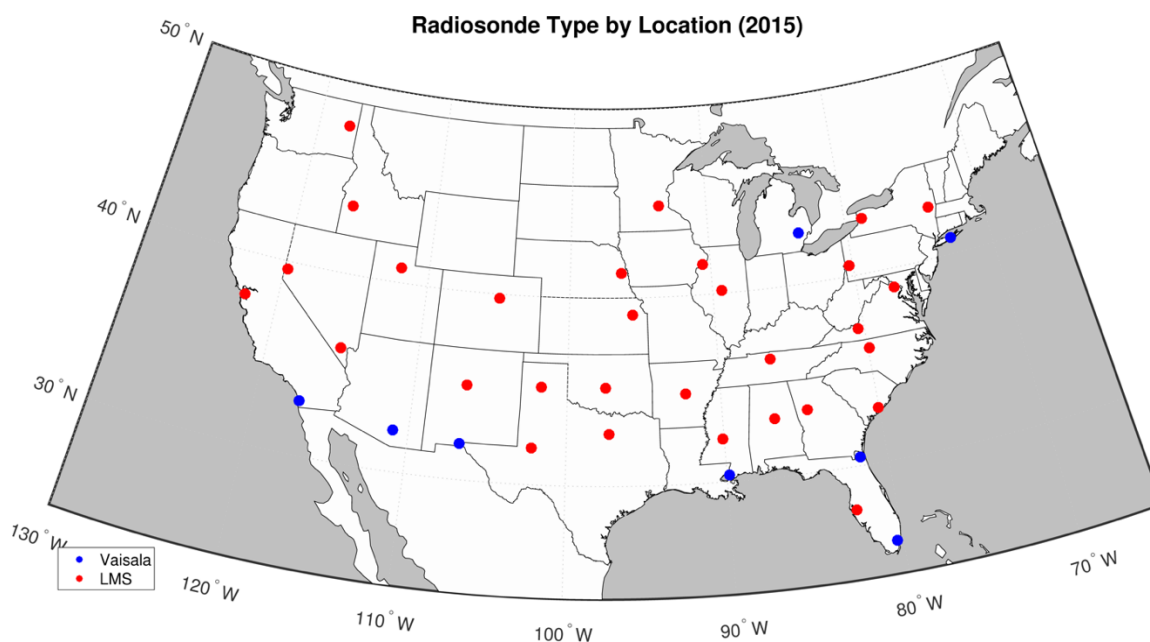


Figure 4.9: Location of the radiosondes types across the CONUS for the comparison locations in this study: Vaisala (blue) and Lockheed Martin Sippican (red).

Examining the individual locations contributing to each of the radiosonde type composites shows how the different locations contribute to the overall average (Fig. 4.10). Figure 4.10 B shows that the few locations contributing to the Vaisala averages all follow the trend of the WVSS-II being drier than the radiosondes in the lowest levels and becoming

slightly moist with increased altitude. On the other hand, the LMS locations (Fig. 4.10 A) have much more variability especially in the lowest levels as expected with more contributing locations. At higher altitudes, the variability decreases. Overall though, most of the individual locations still follow Lockheed Martin Sippican average.

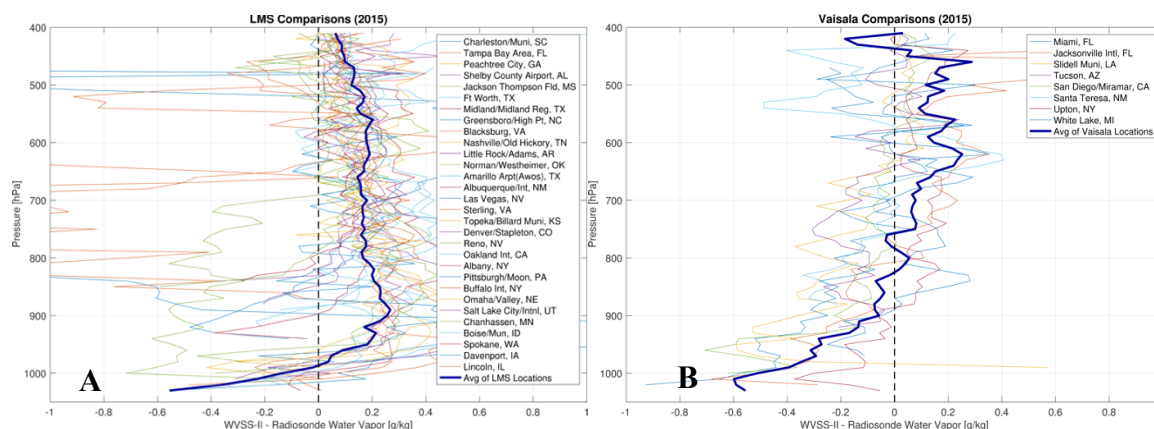


Figure 4.10: All locations 2015 average differences between the WVSS-II observations and the radiosonde type with the radiosonde type average plotted as the thicker navy line. [Lockheed Martin Sippican (A), Vaisala (B)].

Summer had the largest differences of any season. The LMS seasonal differences (Fig. 4.11) similarly follow the same structure as the CONUS comparisons with summertime WVSS-II observations being moister than the radiosondes. As expected, the Vaisala seasons (Fig. 4.12) do not follow the CONUS seasons as closely since only 20% of radiosondes in the CONUS averages are from Vaisala. The Vaisala comparisons have the WVSS-II being drier in the low levels regardless of season with the dry difference being smallest in summer but still quite large for winter, spring, and fall. The WVSS-II observations in winter and spring also are moister from 650 hPa to 450 hPa where the summer moist difference ranges from 900 – 500 hPa which follows the CONUS summer average.

LMS Seasonal Comparisons

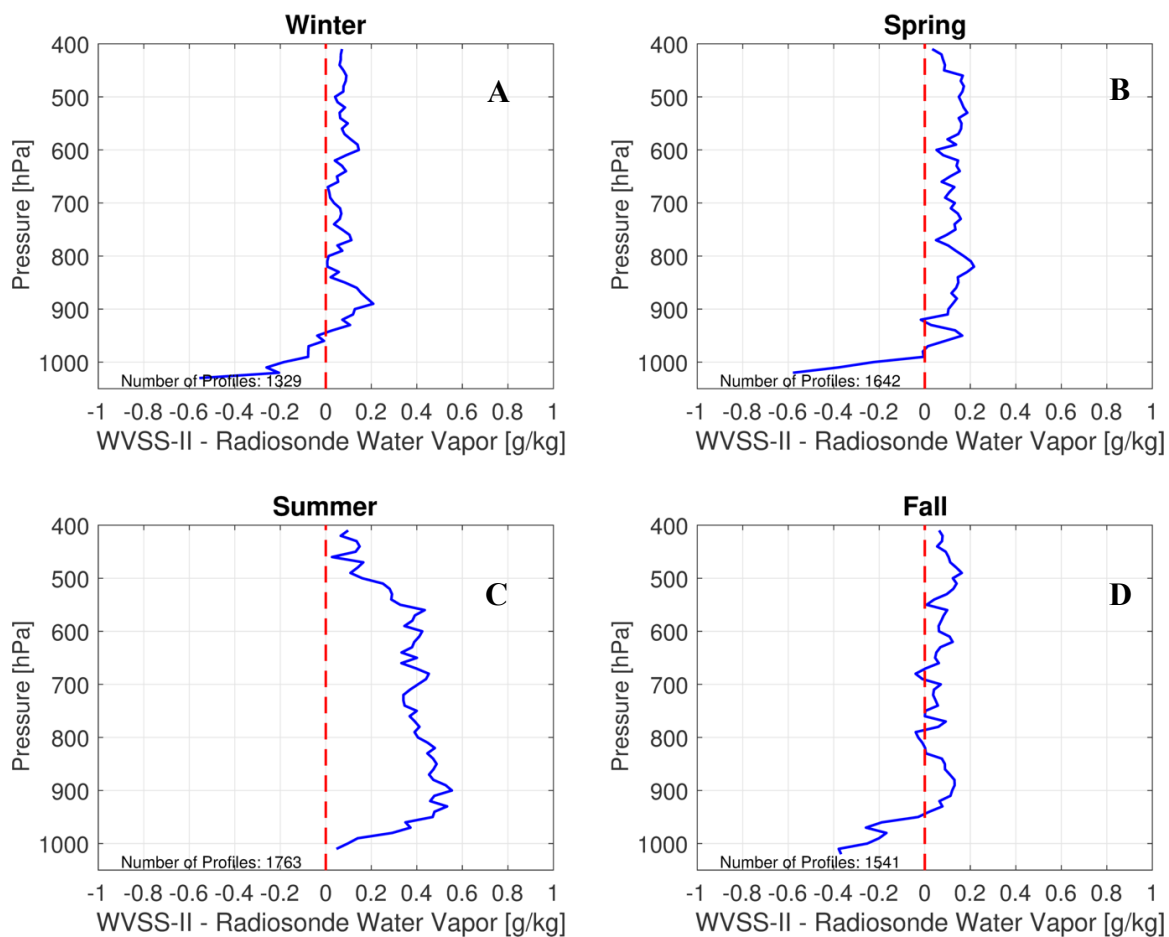


Figure 4.11: Lockheed Martin Sippican radiosondes by season: winter (A), spring (B), summer (C), and fall (D).

Vaisala Seasonal Comparisons

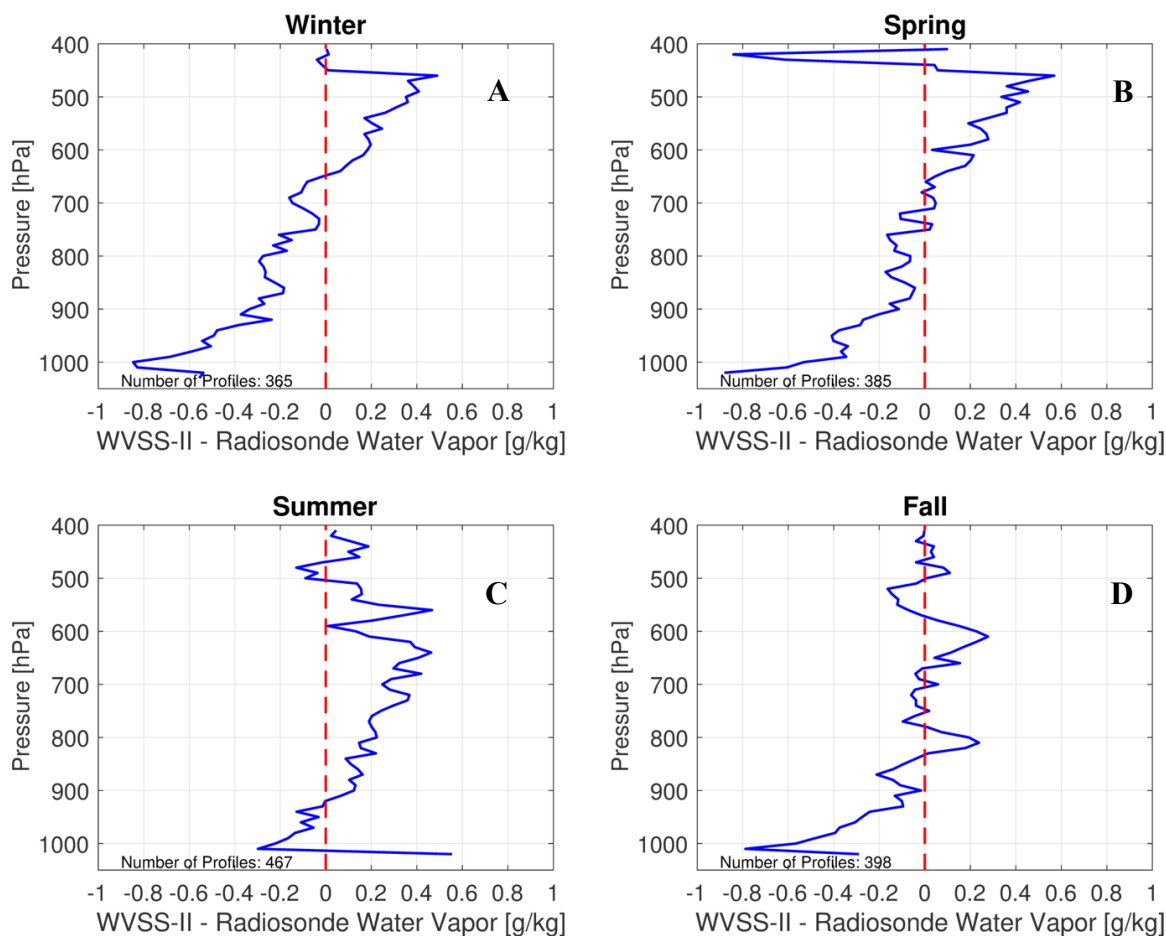


Figure 4.12: Vaisala radiosondes by season: winter (A), spring (B), summer (C), and fall (D).

4.4 Differences above Surface

The lowest levels of the CONUS comparison profile vary with the number of locations contributing the average due to the different surface pressures of each location. To account for this, the average surface pressure was found at each location and differences for 250 hPa above the average surface pressure level were used to create the following difference profiles as a function of pressure above the surface.

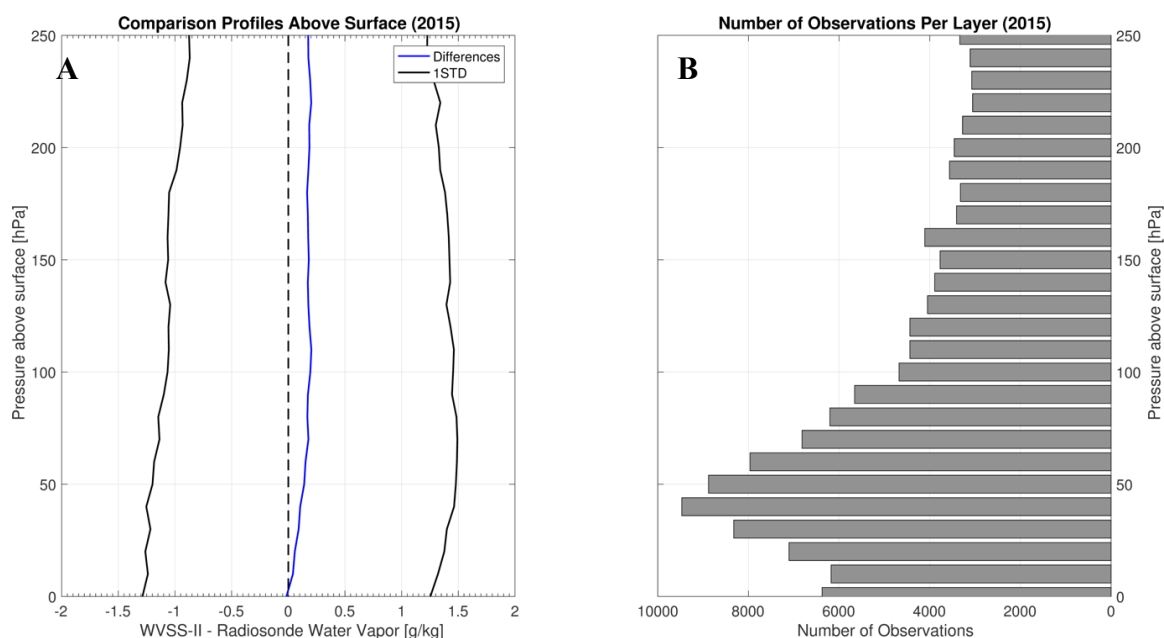


Figure 4.13: Comparison profile as function of pressure above average surface pressure levels (A) and observations per layer (B).

Figure 4.13 shows the comparison profile average as a function of pressure above the average surface pressure. This profile has a similar structure to Figure 4.3 A above 1000 hPa. The WVSS-II is slightly moister than the radiosondes, which increases as the altitude increases with the maximum difference at approximately 0.2 g kg^{-1} . The variability is nearly constant throughout the profile. The maximum number of observations per layer occurs at 40 hPa above the surface and decreases steadily as aircraft and radiosondes get further away from each other. Separating up the WVSS-II observations into ascending and descending datasets shows the observations on descending aircraft have a smaller difference (Fig. 4.14). When above 60 hPa above the surface, the descending differences are half of the ascending differences.

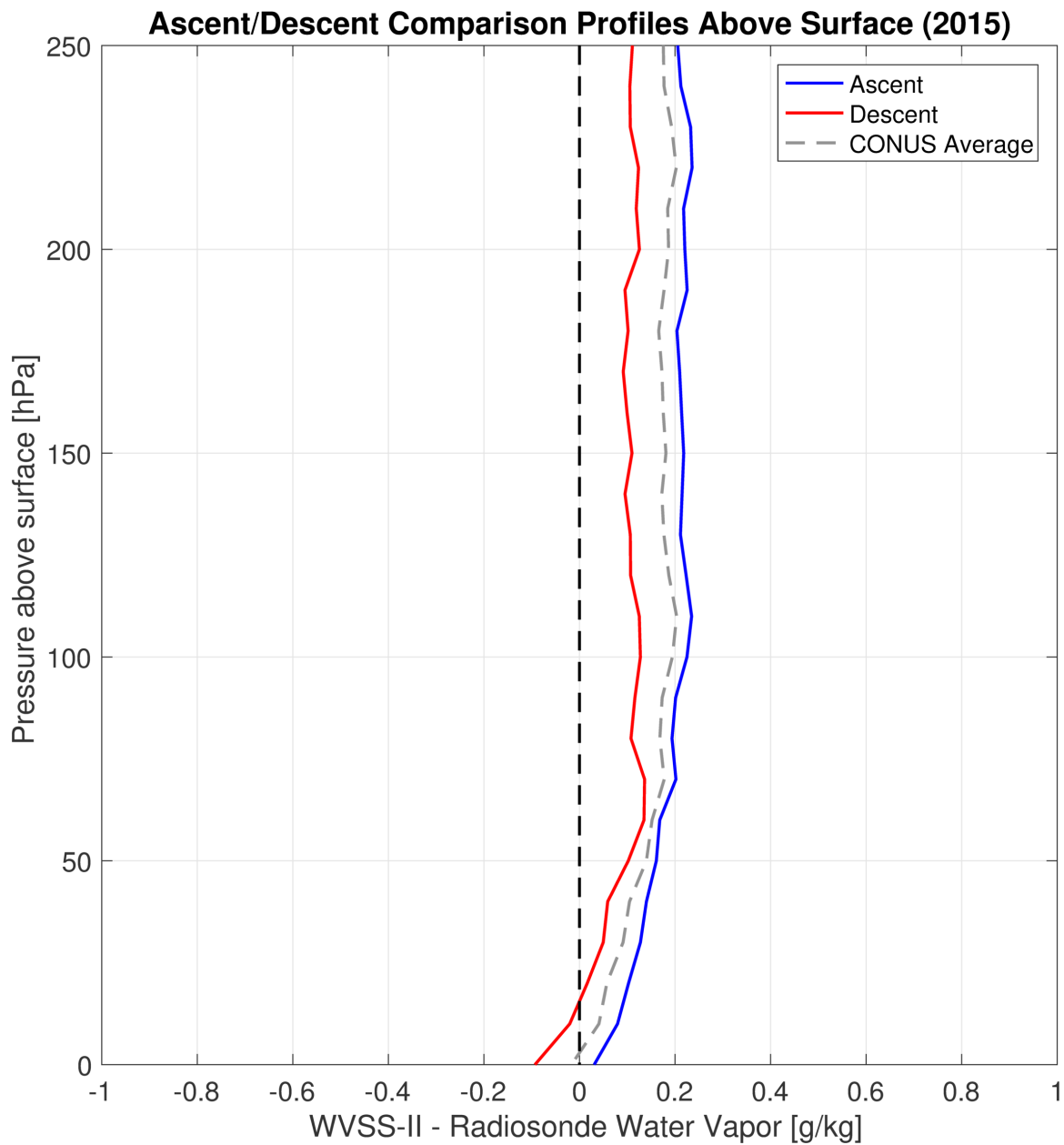


Figure 4.14: CONUS composite of comparison profiles as a function of pressure above the surface comparing WVSS-II observations on during ascent (blue) and descent (red) to the CONUS average (gray dashed).

4.5 700 hPa – 200 hPa Comparisons

In addition to examining how the WVSS-II compares with radiosondes at the lowest levels of the atmosphere, it was also important to see how it compared at higher levels of the atmosphere where aircraft were not necessarily descending or ascending. For these comparisons between 700 hPa and 200 hPa, the WVSS-II observation did not have to originate from an aircraft that was taking off or landing from an airport near the radiosonde launch site, which enables comparisons with observations from aircraft at cruising altitudes flying over the radiosonde launch site. Using the same locations where comparisons were made for the surface – 400 hPa, the CONUS average for 700 – 200 hPa (Fig. 4.15 A) continues to show that the WVSS-II is moister than the radiosondes. The number of observations per level (Fig. 4.15 B) shows the continuation of a decrease in observations per layer from 700 hPa to the minimum in observations at approximately 300 hPa. Above 300 hPa, there is a rapid increase in the number of observations per layer at 200 hPa. Around 200 hPa, aircraft are at cruising altitude, in which aircraft spend much of their time in a single pressure layer.

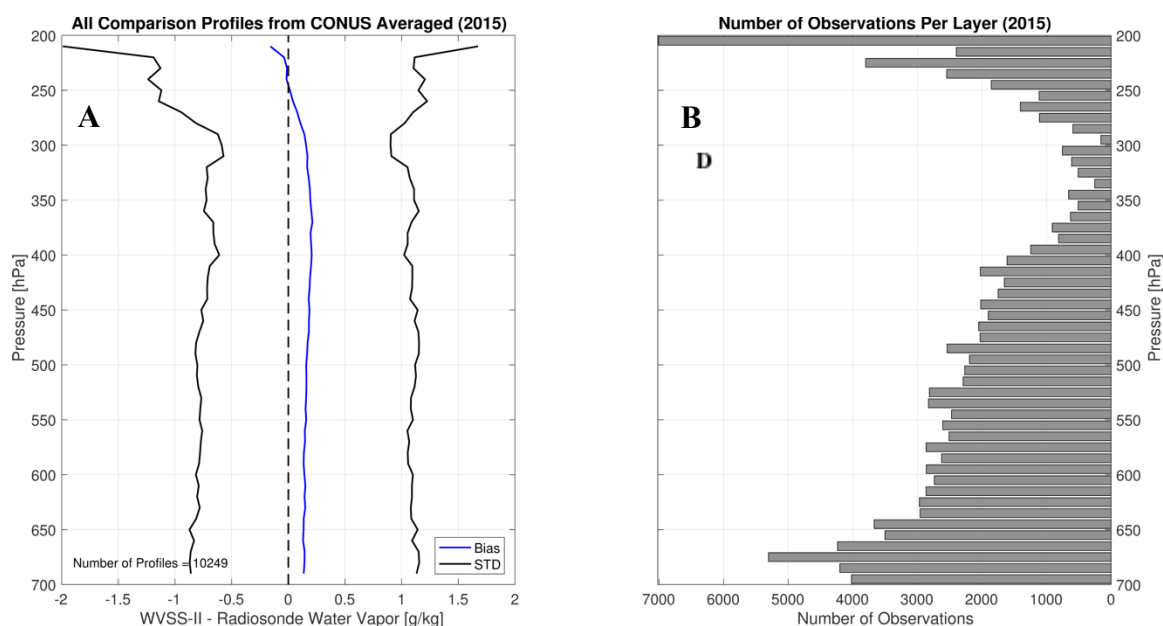


Figure 4.15: 700 – 200 hPa CONUS composite of all comparison profiles with the differences between the WVSS-II and the radiosondes (blue) and two standard deviations (black) (A) and the number of observations for every 10 hPa layer (B).

Throughout most of the profile, the standard deviation is constant until around 300 hPa where it increases rapidly. When the radiosonde temperature sensor is below $-40\text{ }^{\circ}\text{C}$, the response time of the relative humidity sensor decreases and causes less accurate measurements. Figure 4.16 shows the average water vapor profile from both the WVSS-II and the radiosondes as well as the average temperature profile from the radiosondes; note that the $-40\text{ }^{\circ}\text{C}$ level corresponds with the increase in standard deviation just above 300 hPa. The average water vapor mixing ratio profile from the radiosonde shows an obvious error in measurements just below 200 hPa which is also in the region of temperature below $-40\text{ }^{\circ}\text{C}$.

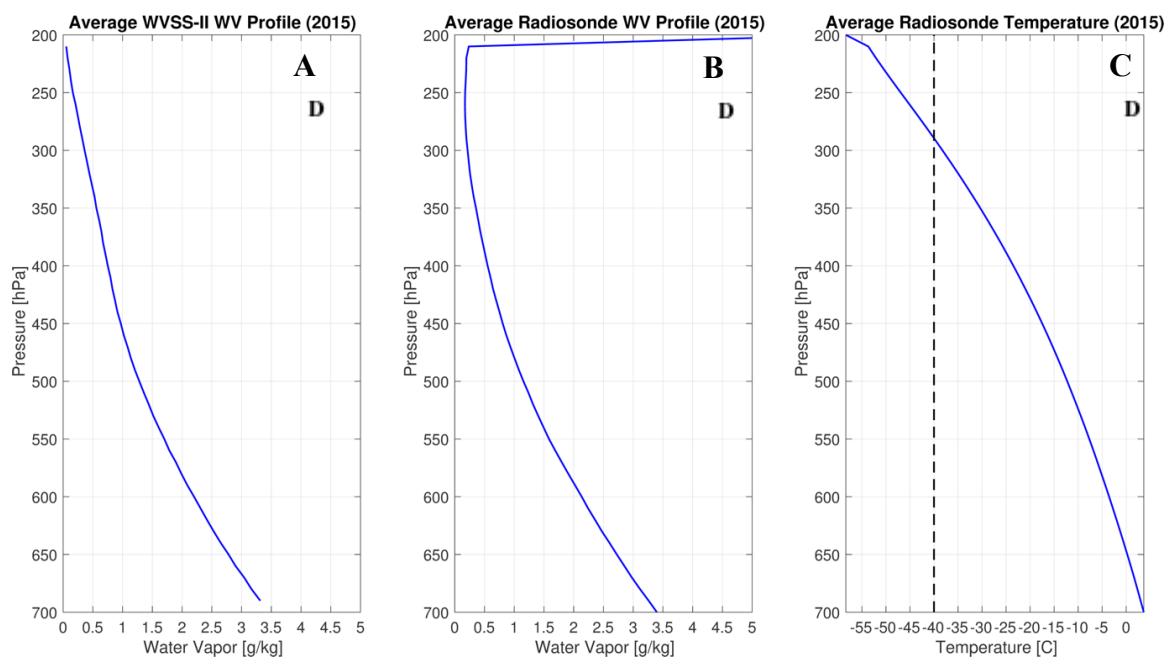


Figure 4.16: Average *WVSS-II* water vapor mixing ratio profile (A), average radiosonde water vapor mixing ratio profile (B), and average radiosonde temperature profile (C).

4.6 Regional Comparisons

Six climate regions defined by the Köppen-Geiger Climate Classification Scheme (Fig. 4.17) were used for the regional comparisons constructed for the surface to 400 hPa pressure range. Table 1 shows the regions with contributing locations. The warm temperate, fully humid, hot summer (Cfa) region is the largest region in area and number of locations. This region is located in the southern/eastern CONUS and is composed of nearly one-third of the locations used for this study. The next largest region is the snow, fully humid, warm summer region (Dfb) and is made up of location in the northern portions of the CONUS. The cold arid, steppe (BSk) region run along the central CONUS and contains three locations. Similar to the BSk region, the cold arid, desert (BWk) region also has three locations but is most spread out. The warm temperate, dry hot summers (Csa) region is along the California

coast with Oakland and San Diego, California. Lastly, Boise, Idaho and Spokane, Washington both lie within two regions; the warm temperate, dry warm summers (Csb) and snow, dry warm summers (Dsb).

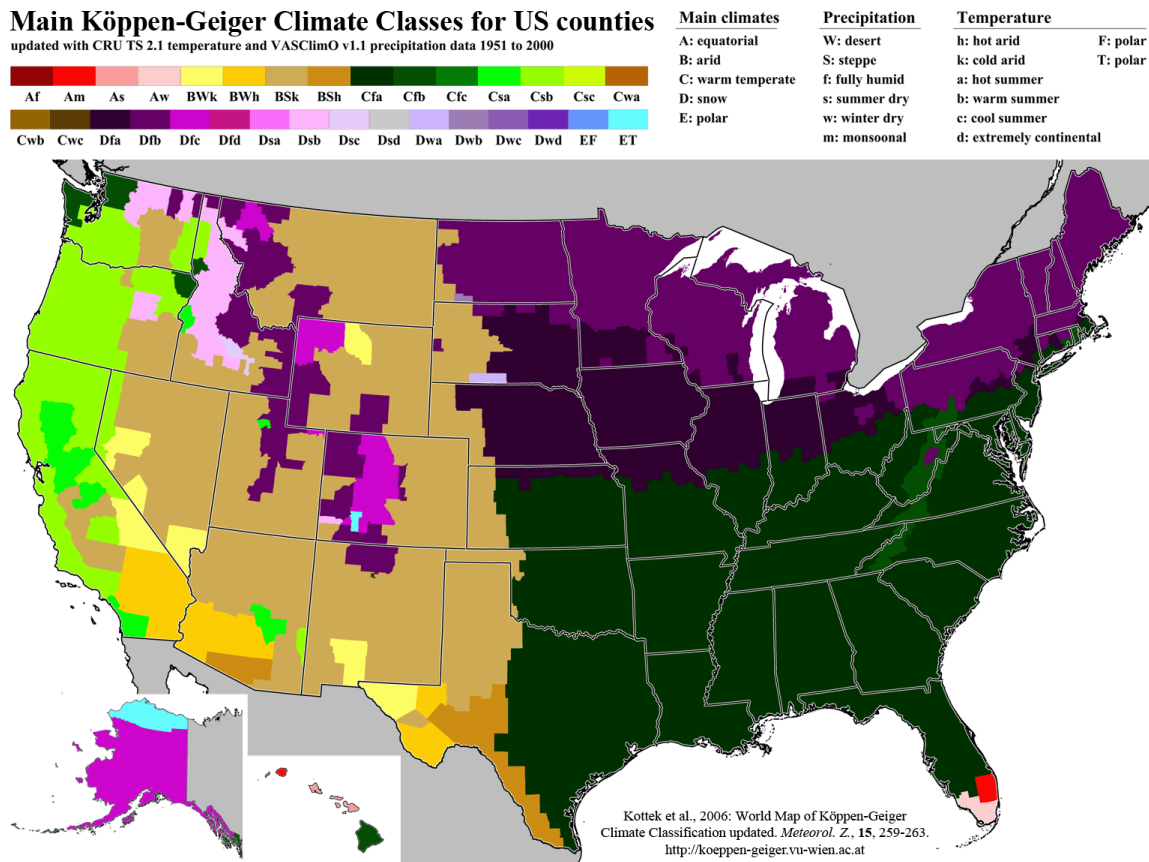


Figure 4.17: The Köppen-Geiger climate classes for the CONUS by county. (Kottek et al. 2006).

Because four of the six climate regions have less than three locations contributing to the regional average, larger regions were formed from the six regions based off the precipitation classification from the Köppen-Geiger Climate Classification. The Cfa and Dfb regions were combined to form the fully humid East Region, the BSk and BWk regions were

combined to form the steppe/desert Mountain/Desert Region, and lastly, the Csa and Csb/Dsb regions were combined to form the dry summer West Region.

Regional comparisons were made by finding the location within the region with the lowest number of comparisons and randomly selecting that number of comparison profiles from each of the other locations within the region. All of those comparisons profiles selected were then averaged for the region to form the regional average.

The regional averages (Fig. 4.18) indicate the largest variability in the lowest levels. Above 800 hPa, all regions show good agreement with the WVSS-II being moister than the radiosondes. Examining the individual regions in more depth shows how the individual locations contribute to the region as a whole. The East Region (Fig. 4.19) is the largest region in both the area covered and the number of locations contributing to the average. Overall, the regional average follows the CONUS average previously mentioned with the WVSS-II being moister above 1000 hPa. As before, the largest variability is in the lowest levels but as pressure decreases, the variability decreases. The Mountain/Desert Region has less locations contributing to the average and the surface at a lower pressure due to the higher elevation of these regions. This region shows a slightly different structure (Fig. 4.20) than the East Region with the WVSS-II being slightly drier than the radiosondes at the lowest levels.

Table 1: Locations with comparison profiles contributing to each region.

Warm temperate, fully humid, hot summer (Cfa)	Snow, fully humid, warm summer (Dfb)	Cold arid, steppe (BSk)	Cold arid, desert (BWk)	Warm temperate, dry hot summer (Csa)	Warm temperate / snow, dry warm summer (Csb/Dsb)
Upton, NY	Albany, NY	Denver, CO	Las Vegas, NV	Oakland, CA	Boise, ID
Sterling, VA	Buffalo, NY	Tucson, AZ	El Paso, TX	San Diego, CA	Spokane, WA
Charleston, SC	Chanhassen / Minneapolis, MN	Albuquerque, NM	Reno, NV		
Jacksonville, FL	White Lake / Detroit, MI				
Slidell, LA					
Atlanta / Peachtree City, GA					
Little Rock, AR					
Norman, OK					
Dallas – Fort Worth, TX					
Tampa Bay, FL					
Birmingham, AL					
Nashville, TN					

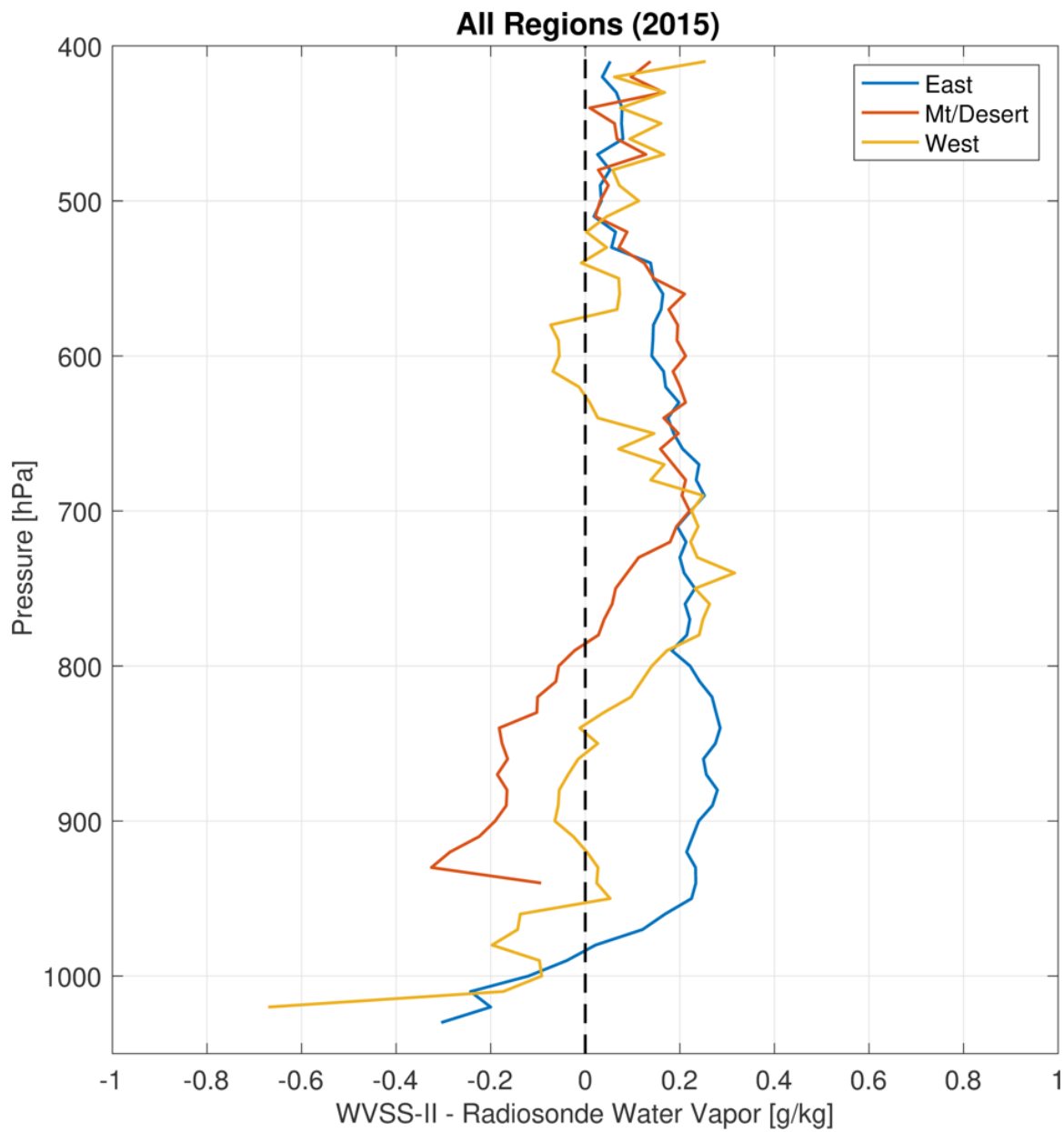


Figure 4.18: The regional averages from the East (blue), Mountain/Desert (red) and West (yellow) regions.

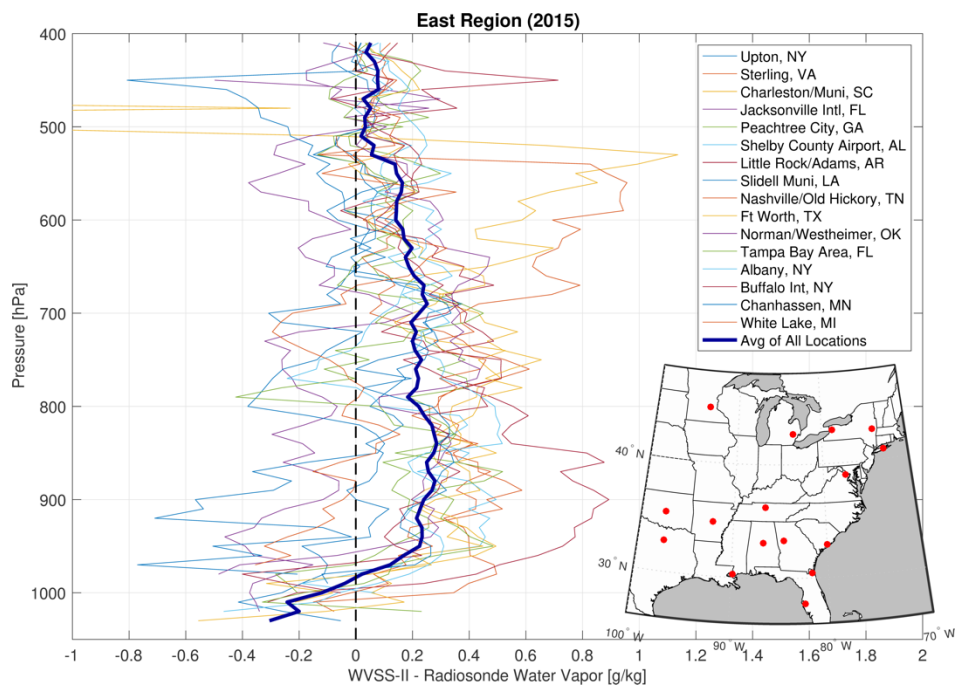


Figure 4.19: The fully humid East Region average with each location's average contributing to the region and the inset showing the cities' locations.

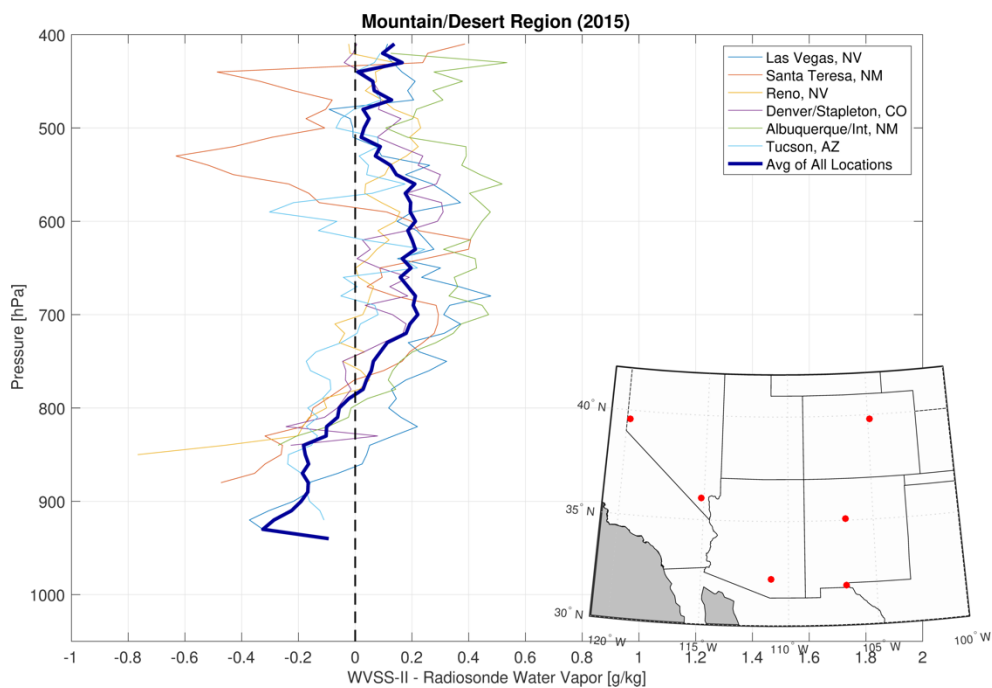


Figure 4.20: Same as Figure 4.19 but for the Mountain/Desert Region.

4.7 UPS Only Comparisons

Comparisons were made using WVSS-II observations from only UPS aircraft. These differ from the Southwest aircraft that form the bulk of dataset in several significant ways. First, the UPS mounts its WVSS-II sensors exclusively to Boeing 757s, while Southwest's entire fleet is composed of 737s. Second, UPS aircraft tend to operate at night to facilitate overnight shipping and take advantage of reduced traffic at its hub airports. Finally, the landing and takeoff profiles tend to be much sharper as UPS pilots do not need to worry about passenger comfort. To maintain corporate privacy and security, the publicly accessible AMDAR dataset does not contain identifiable airlines, flight numbers, or aircraft tail numbers, although every individual aircraft has a unique encrypted tail number in the dataset. Therefore, an alternative method to identifying UPS aircraft was developed. UPS's hub of operations is in Louisville, Kentucky, where over 100 airplanes converge nearly every night in order to rapidly exchange packages; few other planes visit Louisville during the overnight hours in which UPS is active. A convenient way to identify the UPS planes is to merely look at the aircraft frequently landing at or departing from Louisville between the hours of 0500 UTC and 0900 UTC. UPS planes were selected as those which were in the top 75 percentiles of frequency of visits to Louisville during those hours. It is possible that this sorting technique does not capture every UPS aircraft, but the resulting dataset will be largely distinct.

UPS comparisons cannot be done at Louisville since there is no radiosonde site there and most flights are not during the synoptic launch hours. Instead, they are all around the country with the largest number of comparisons at Miami, Florida, and Washington D.C. (Fig. 4.21 - top) while non-UPS comparisons occur in nearly all the same locations but in

greater magnitude (Fig. 4.21 – bot). The number of comparison profiles for the UPS aircraft are approximately 10% of the non-UPS comparisons. The only UPS average profile differences are slightly more dry than the non-UPS comparisons below 850 hPa, nearly zero from 850 hPa and 700 hPa and follow the non-UPS comparisons above 700 hPa. The standard deviations are slightly larger for the UPS aircraft than the non-UPS aircraft (Fig. 4.22). The WVSS-II is moister than the radiosondes above approximately 1000 hPa and the number of observations per layer is similar for both (not shown).

Similar to previous sections, the ascending and descending UPS/non-UPS aircraft were also evaluated separately (Fig. 4.23). These results are comparable to before with the WVSS-II observations on ascending aircraft being moister than radiosonde than descending observations. For descending aircraft, the differences between the WVSS-II and the radiosondes are drier than the radiosondes below 600 hPa while for ascending aircraft the differences follow the non-UPS profiles and are moister from 900 hPa and 750 hPa. Below 1000 hPa, both the ascending and descending WVSS-II observations are much drier than the radiosondes.

Most UPS flights fly overnight to ship packages so the differences between the 0000 UTC and 1200 UTC comparisons were also completed (Fig. 4.24). Overall, comparisons at 1200 UTC and 0000 UTC have the same structure for UPS aircraft with 1200 UTC comparisons are moister than the 0000 UTC from approximately 900 hPa to 750 hPa. The 0000 UTC and 1200 UTC comparison profiles for the non-UPS aircraft follow the same structure.

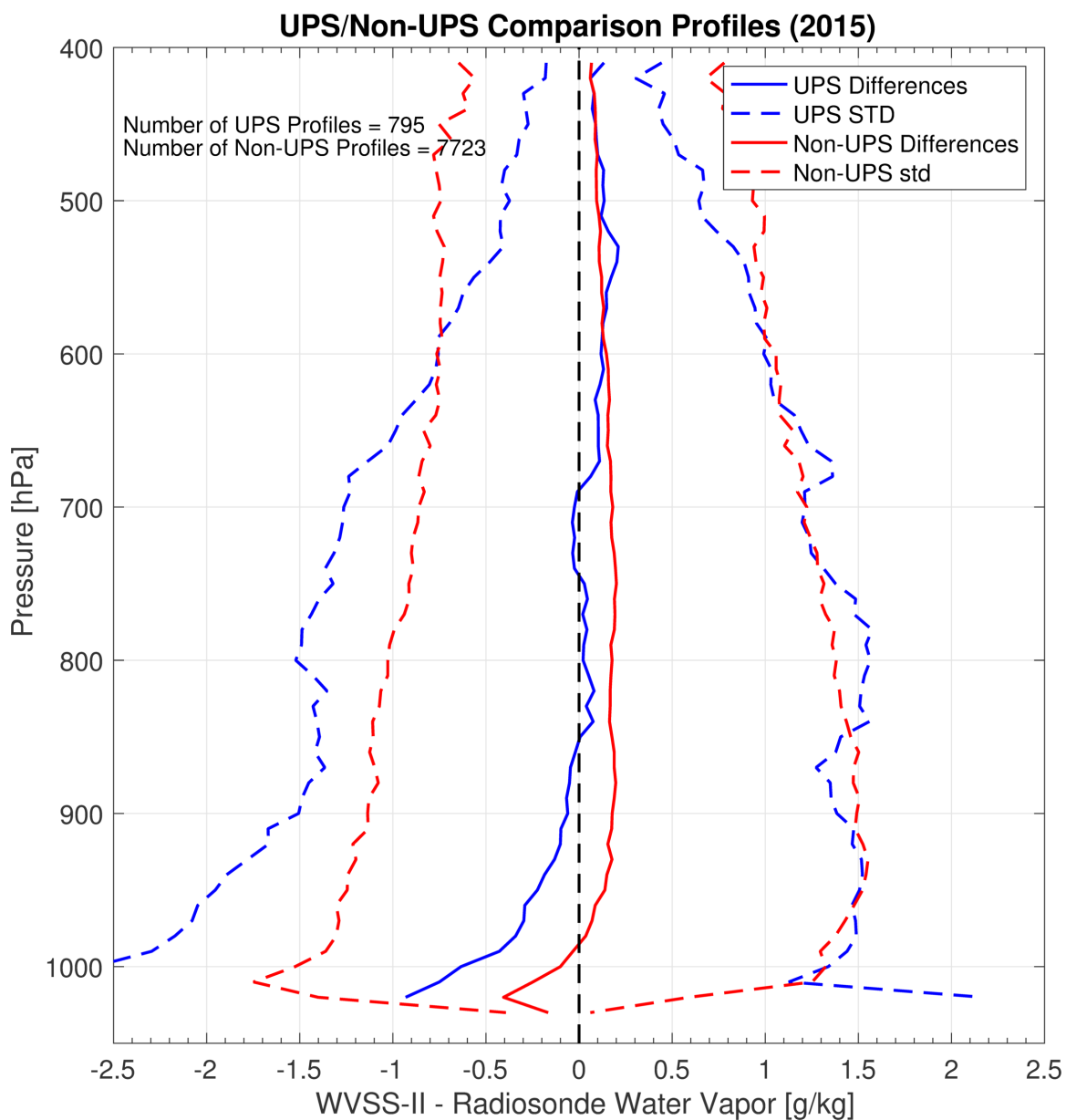


Figure 4.22: CONUS composite of comparison profiles using only WVSS-II observations for UPS aircraft (blue), one standard deviation for UPS aircraft (blue dashed), non-UPS aircraft (red), and one standard deviation for non-UPS aircraft (red dashed).

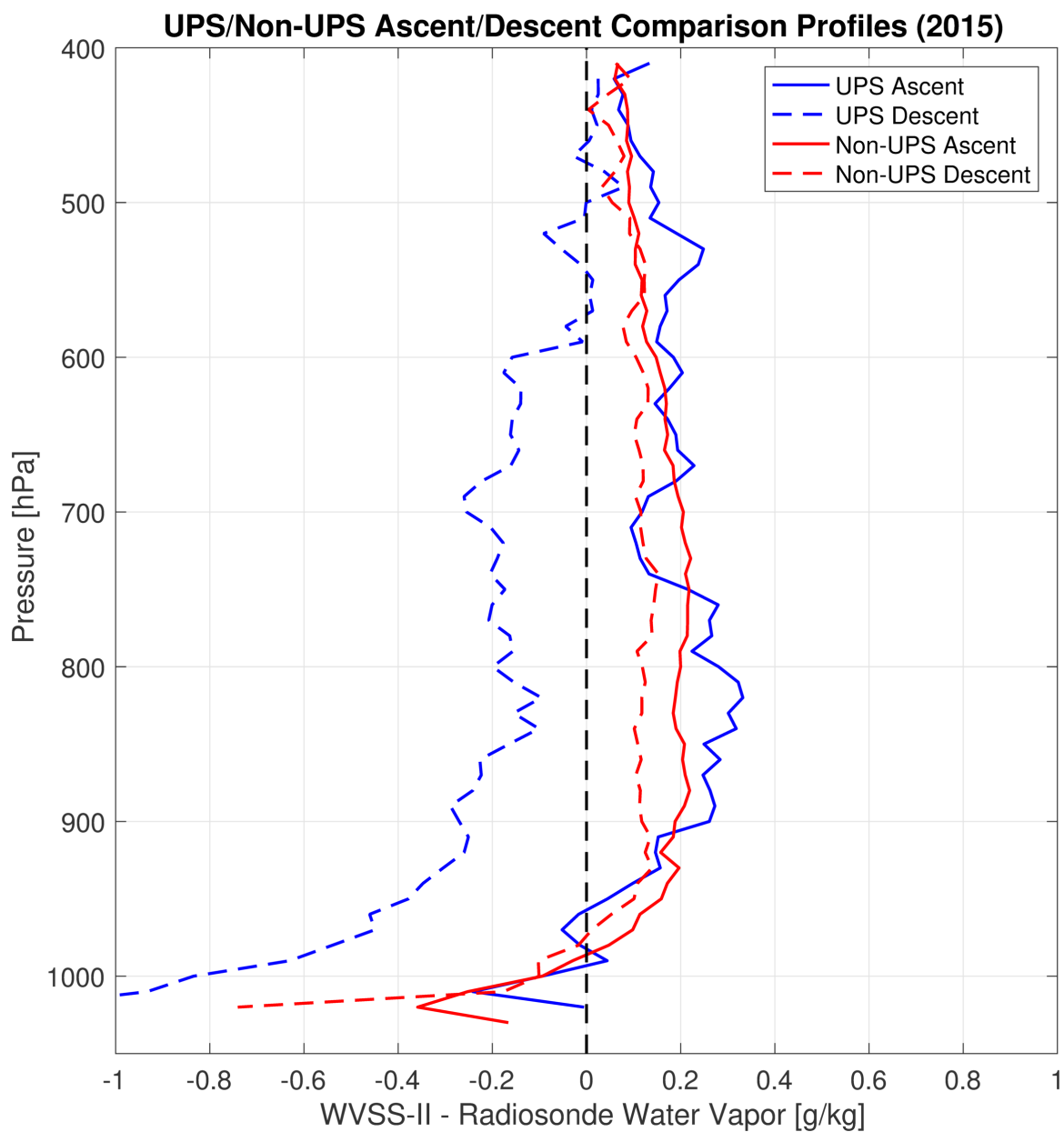


Figure 4.23: Comparisons profiles for WVSS-II observations from ascending UPS aircraft (blue), descending UPS aircraft (blue dashed), ascending non-UPS aircraft (red), and descending non-UPS aircraft (red-dashed).

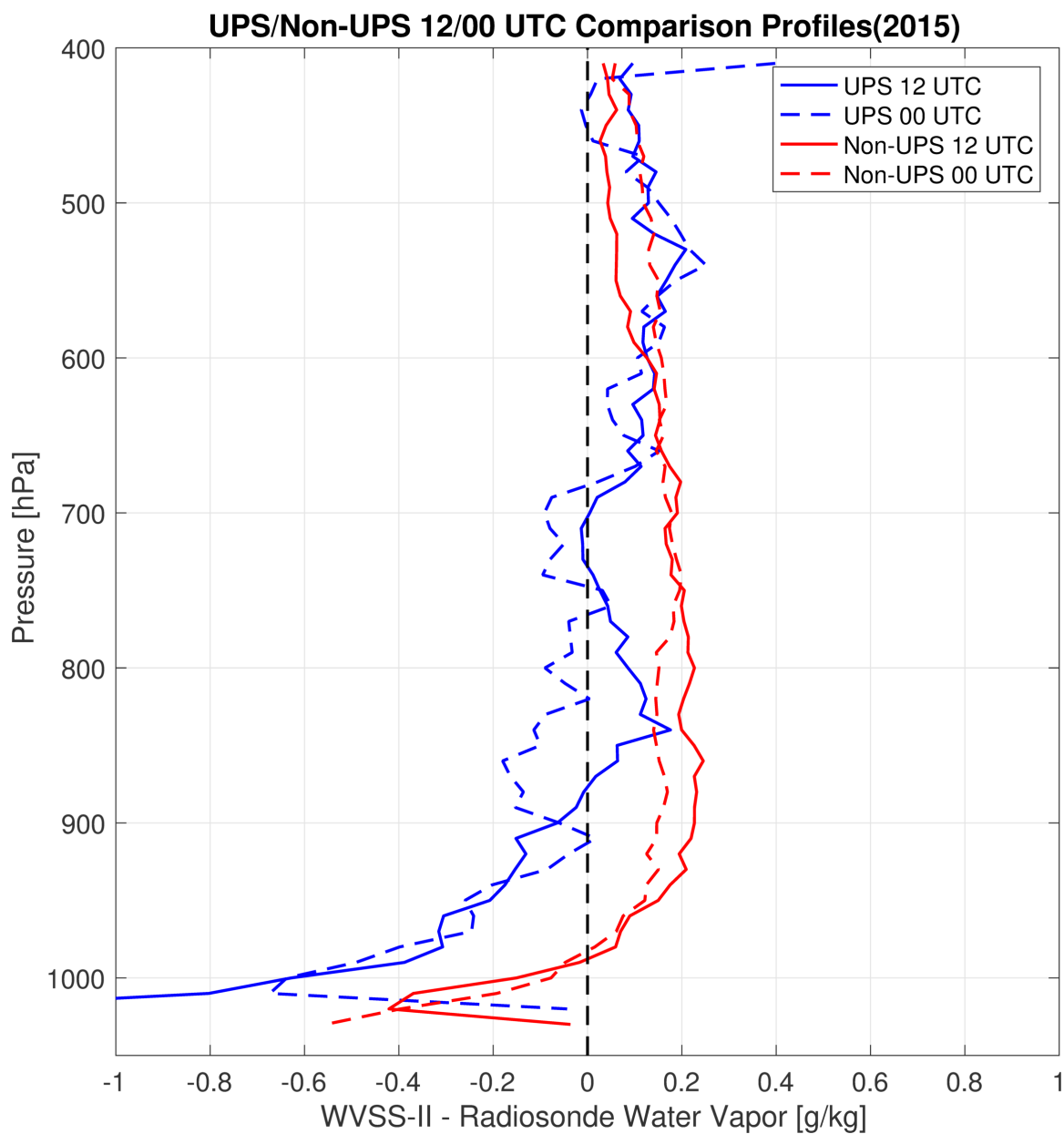


Figure 4.24: Comparisons profiles from only UPS aircraft at 1200 UTC (blue) and 0000 UTC (blue dashed) and for Non-UPS at 1200 UTC (red) and 0000 UTC (red dashed).

4.8 Individual Locations

Two climatologically different locations were examined for the whole year and then by seasons to see how individual locations with climatologically different amounts of water

vapor present in the atmosphere compare with each other. The locations chosen were Las Vegas, Nevada, and Tampa Bay, Florida. Both locations have over 300 comparison profiles for 2015 and both use the LMS6 radiosonde model. Las Vegas, NV is in the cold arid desert Köppen-Geiger climate class and Tampa Bay, FL is considered to be warm temperate, hot summers, and fully humid.

Las Vegas, NV (Fig. 4.25) shows the WVSS-II being slightly dry at the lowest levels and then being slightly moist from 800-400 hPa when compared with the radiosondes. The average water vapor content maximum is less than 5 g kg^{-1} and the variability is around 1 g kg^{-1} for most of the profile. Winter shows the smallest magnitude of differences while summer has the largest.

By comparison, Tampa Bay, FL has a water vapor content maximum near 15 g kg^{-1} , over three times larger than Las Vegas (Fig. 4.26). The difference profile is not nearly as smooth as the profile for Las Vegas and follows the CONUS composite of difference much more closely with the WVSS-II being slightly moist below 600 hPa. The variability is much larger with the largest variability at the lowest levels and decreasing slightly with increased altitude. When looking at the individual seasons, winter follows the zero difference line, with a slight moist difference in spring and a slight moist difference in the lowest levels of fall. Summer has the largest moist difference below 650 hPa with a dry difference from 550 hPa – 450 hPa. From these two locations, as well as the regional comparisons, the variability of the WVSS-II measurements most likely depends on the amount of water vapor present in the atmosphere.

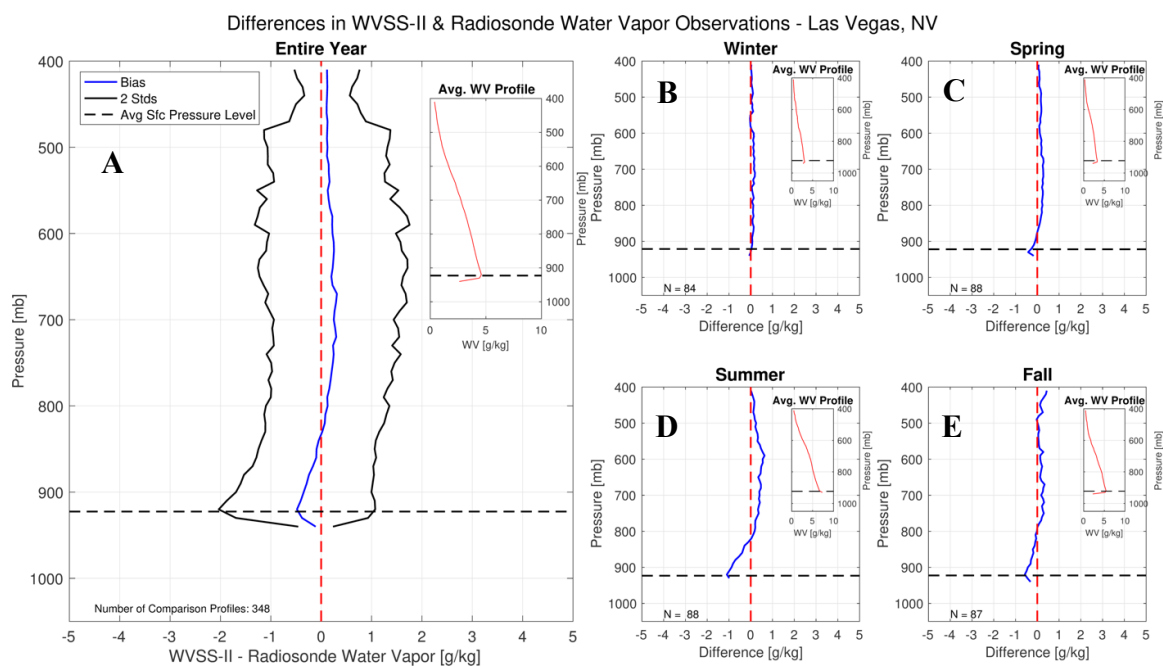


Figure 4.25: All comparison profiles of differences (blue) from Las Vegas, NV averaged for 2015 with two standard deviations (black) (A) and then divided by seasons: winter (B), spring (C), summer (D), and fall (E). The inset in each plot shows the average water vapor profile from the radiosondes for that time period. The black dashed line shows the average surface pressure collected from the radiosondes for the whole year.

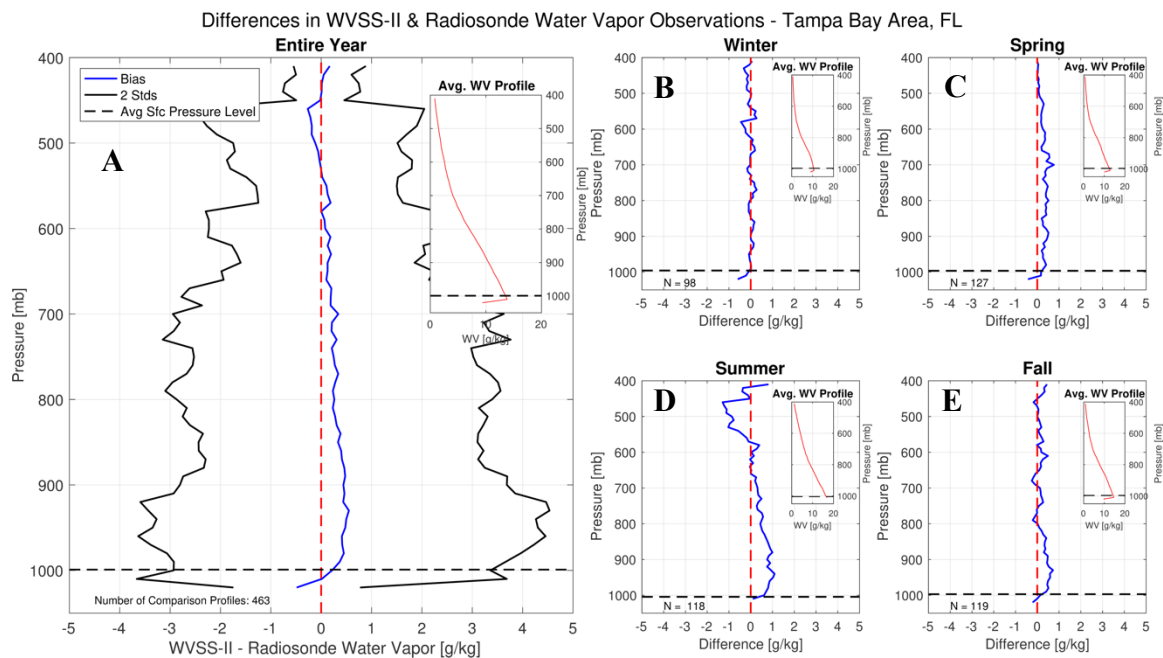


Figure 4.26: Same as Figure 4.25 but for Tampa Bay, FL.

4.9 Individual Aircraft Comparisons

Comparisons between the WVSS-II and the radiosondes were made for a single plane to evaluate the noise of an individual sensor (Fig. 4.27). In this case, it was for a UPS aircraft with the greatest number of observations for the year. The comparison profile average showed the WVSS-II being moist compared to the radiosondes from 1000 hPa to 900 hPa and again from approximately 650 hPa to 500 hPa. Between 900 hPa and 650 hPa, the differences are nearly zero with the standard deviation also being at a minimum. The number of observations per level is at a maximum around 920 hPa and steadily decreases as pressure decreases. The locations of the comparisons were still across the CONUS with comparisons made from the Northeast to the west coast as well (Fig. 4.28).

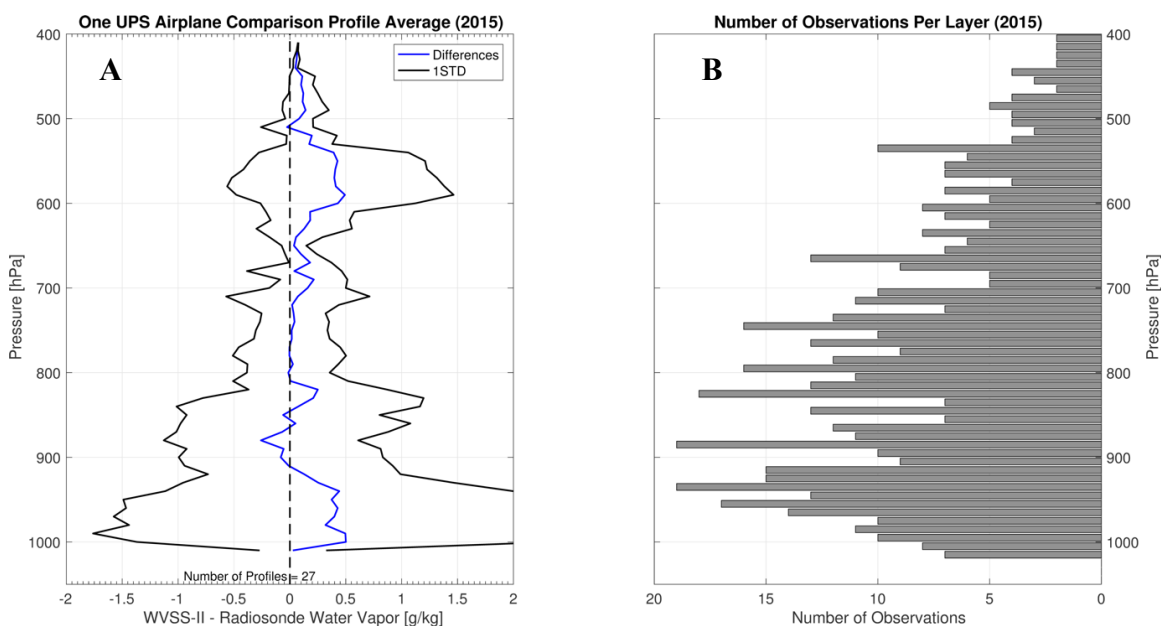


Figure 4.27: CONUS composite of comparison profiles using only WVSS-II observations from one aircraft with the differences between the WVSS-II and the radiosondes (blue) and two standard deviations (black) (A) and the number of observations for every 10 hPa layer (B).

Figure 4.29 shows the comparisons again split up by WVSS-II observations on ascents and descents. Below 850 hPa, the descent comparisons show the WVSS-II being drier than the radiosondes by as much as 0.4 g kg^{-1} whereas the ascent comparisons show the WVSS-II being moister by more than 0.3 g kg^{-1} from the surface to 850 hPa. Above 850 hPa, the differences decrease for both ascending and descending comparisons until 600 hPa. From 600 hPa – 550 hPa, the descent comparisons show a strong moist difference whereas the ascent shows the WVSS-II being moister by 0.2 g kg^{-1} to 0.4 g kg^{-1} . It is important to look at the number of observations per layer at this level. Figure 4.30 shows the number of observations for descent comparisons from 600 hPa – 550 hPa is only about one observation per 10 hPa layer whereas for ascent comparisons there are anywhere between three and six

observations. This could indicate that the large difference in the descent profile at this level is due to one bad comparison rather than a set of bad comparisons.

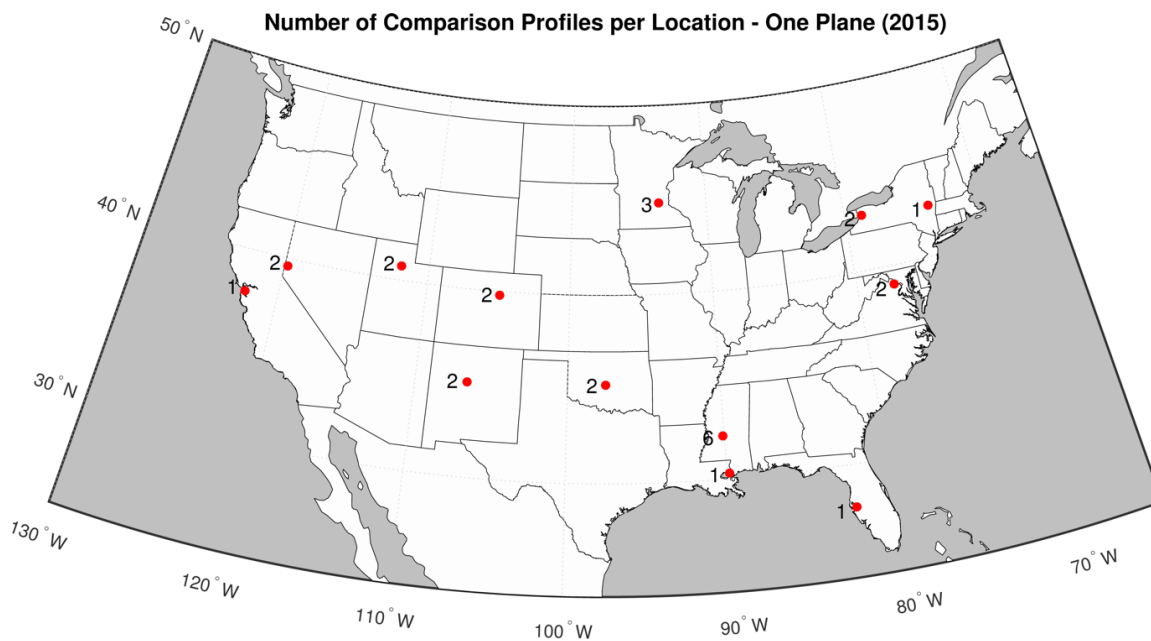


Figure 4.28: Locations of all the comparison profiles from one aircraft.

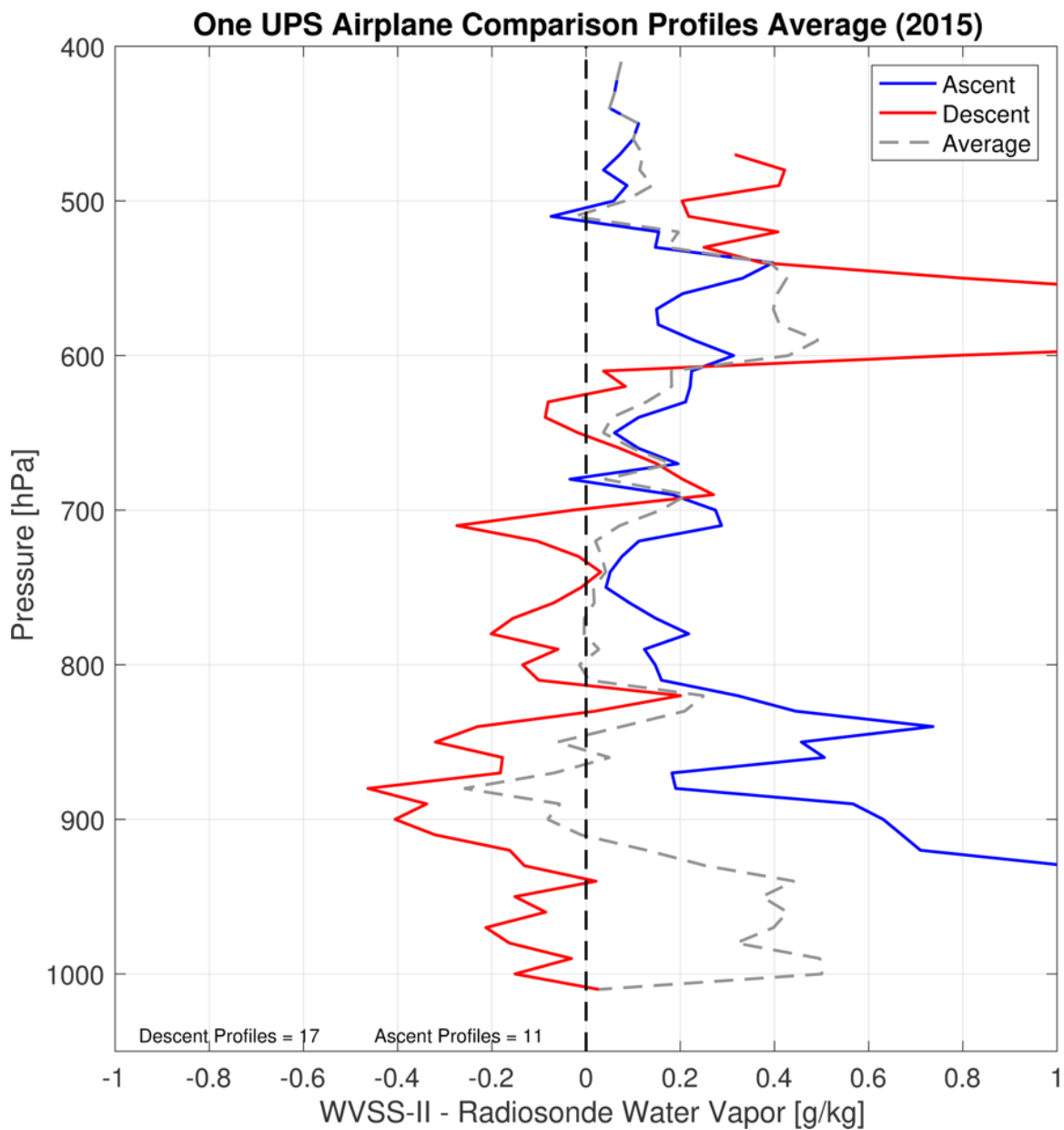


Figure 4.29: Comparisons for one aircraft for ascending (blue) observations and descending (red) observations with the average (gray-dashed).

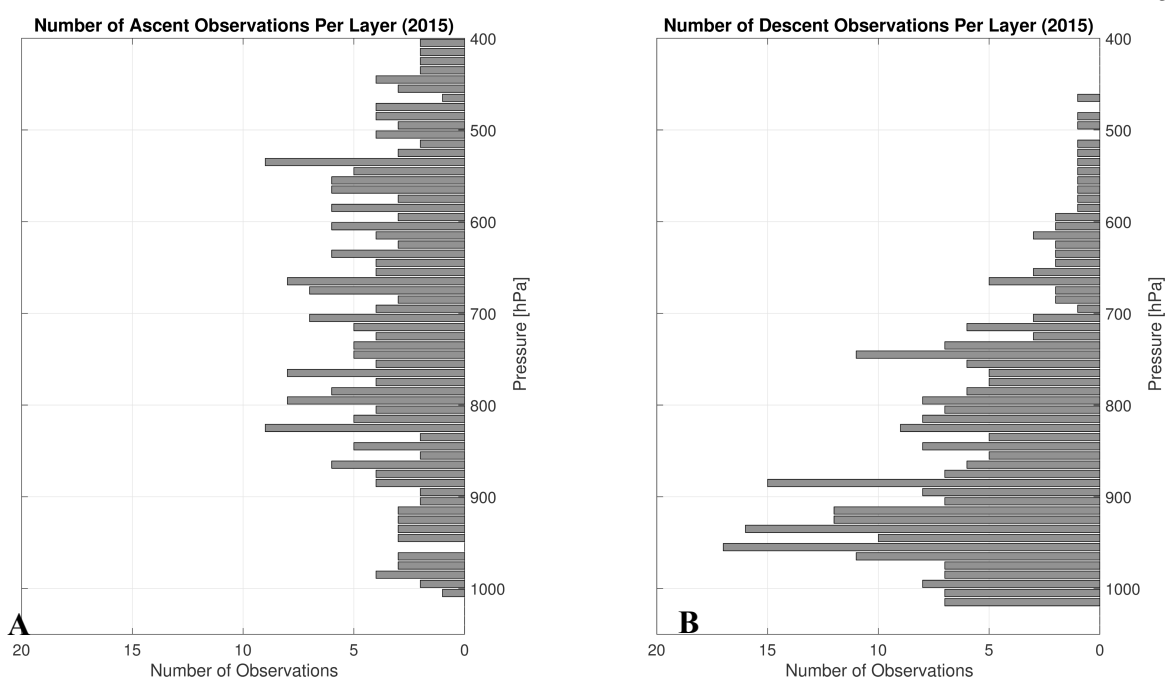


Figure 4.30: : Number of observations per level for one aircraft for ascending observations (A) and descending observations (B).

4.10 Precipitation Profiles versus Clear Profiles

Moisture inside the sensor can lead to increased differences when compared to radiosondes. From that, it stands to reason that precipitation can also impact the magnitude of the differences in similar ways. To examine how precipitation affected the sensor, six cases of when the airplane would most likely have traveled through precipitation were compared with six cases when the airplane traveled through clear skies and minimal clouds; all cases were selected from Atlanta, Georgia. Cases were identified through visual inspection of radar reflectivity imagery (for precipitating cases) and visible satellite imagery (for clear cases). Two precipitating cases and two clear cases were selected for each of the months of March, April, and May (Table 2).

Table 2: List of precipitation cases and clear cases out of Atlanta/Peachtree City, GA.

Precipitation Cases	Clear Cases
22 March 2015 00 Z	8 March 2015 00 Z
23 March 2015 00 Z	29 March 2015 00 Z
7 April 2015 00 Z	5 April 2015 00 Z
17 April 2015 00 Z	22 April 2015 00 Z
27 May 2015 00 Z	2 May 2015 00 Z
29 May 2015 00 Z	23 May 2015 00 Z

Figure 4.31 shows how the precipitating cases and the clear cases compare. The WVSS-II is much moister than the radiosondes when the aircraft fly through precipitation than when they fly through clear skies. On average, for most pressures, the precipitation average is around 1 g kg^{-1} greater than the clear average. The variability of the precipitation cases is also larger whereas the clear cases tend to be more focused around the average; however, this is for a much smaller sample size than previous subsets of the data examined.

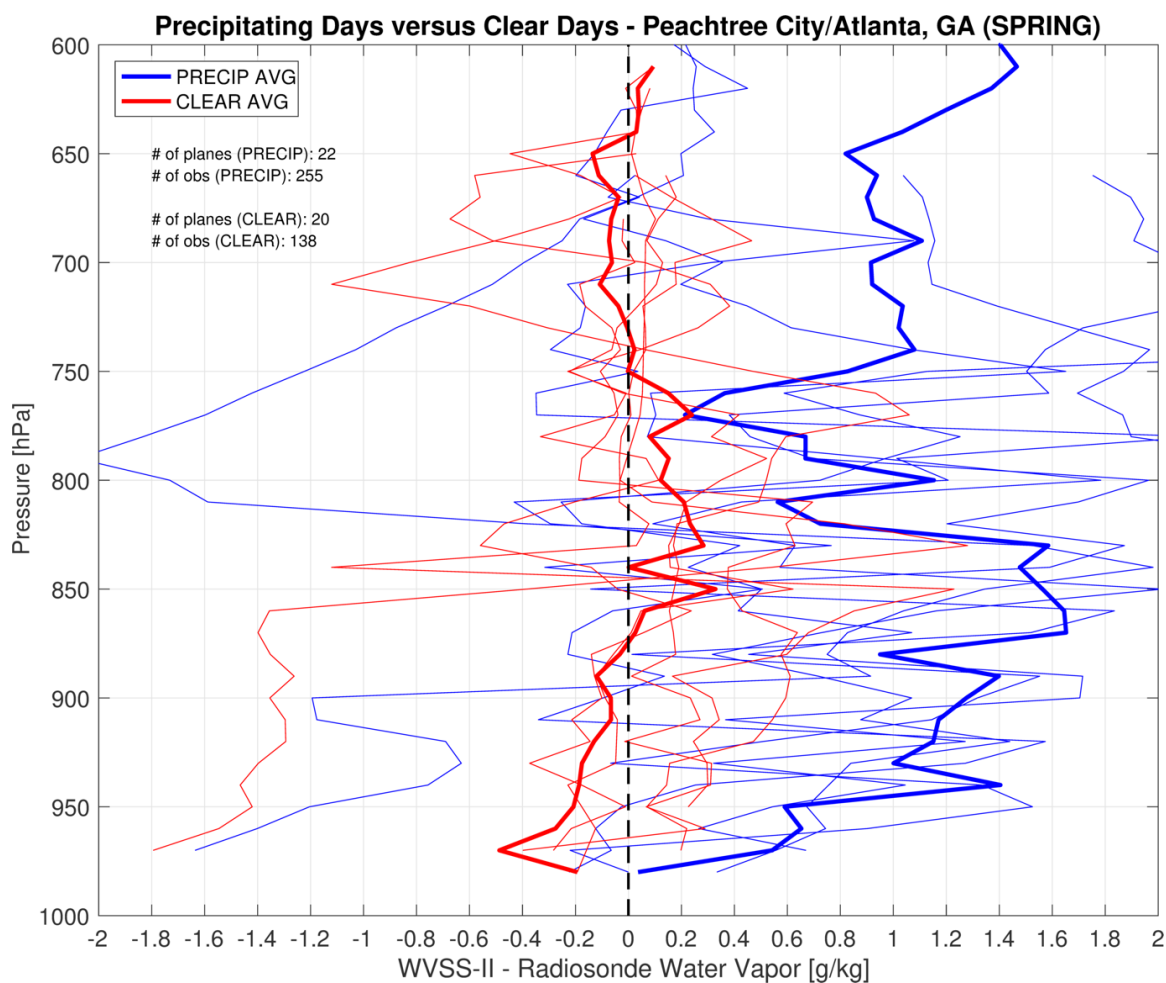


Figure 4.31: Individual cases plotted in the thinner lines with the average of the precipitating cases (blue) and clear cases (red) in the thicker lines.

This finding of the larger moist difference with precipitation could explain why the WVSS-II is moister when compared with radiosondes on the CONUS scale throughout most of the atmosphere. Because there is a moist difference for precipitation cases and no countering effect causing a dry difference, when all these cases are averaged together, it could cause the slight moist difference for the CONUS composite.

For these particular cases, most of the observations originate from descending aircraft whereas only a handful of aircraft form the ascending averages (Fig. 4.32). Even only having

one profile from the clear cases for the ascending, both ascending and descending observations show the WVSS-II observations going through precipitation being moister than the radiosondes.

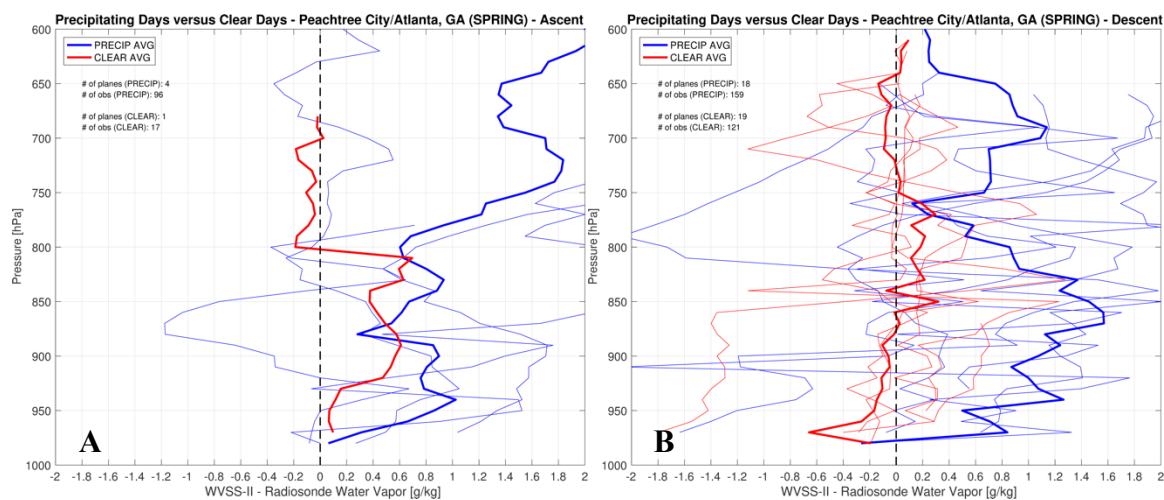


Figure 4.32: Same as previous figure but for ascending WVSS-II observations (A) and descending observations (B).

4.11 Discussion of Differences

Differences between the WVSS-II could be due to a number of different reasons. Many studies have noted that the WVSS-II has a very fast response time by using a laser diode (Fleming and May 2004; Helms et al. 2010). If the WVSS-II is responding faster than the radiosonde as they both travel through the same environment, the radiosonde would contain a lag. This lag would be contributing to differences found between the WVSS-II and the radiosonde while each sensor still performs to its standard.

Other causes for the differences could be that water vapor is highly variable in space and time. Examining the differences within 50 km and 10 hPa, gradients could still exist

within the boundaries which would still result in large differences between the WVSS-II and the radiosondes. Biases that already exist in radiosondes could be another contribution to the differences when compared with the WVSS-II.

5 Conclusions

With the development of the WVSS-II, water vapor measurements have been added to the preexisting pressure, wind, and temperature observations that are routinely taken by commercial aircraft during flight. While limited studies have been conducted, no study thus far has examined how the sensor preforms in different climates and distinct seasons. The frequent collocation of operational radiosondes and WVSS-II equipped aircraft enables such a study. Comparisons were made for two pressure ranges: surface – 400 hPa and 700 – 200 hPa. For comparisons from the surface – 400 hPa, ascent versus descent, radiosonde model, regional response, UPS aircraft, individual locations, an individual aircraft, and precipitation versus clear days were investigated.

For the comparisons from the surface – 400 hPa, the WVSS-II was slightly moist for most of the profile above 1000 hPa with summer having the largest moist difference, and winter with the smallest. The WVSS-II observations from descending aircraft have less than half the difference of the observations from ascending aircraft from 950 hPa – 600 hPa. These differences could be caused by ascending aircraft flying from moist environments to more dry environments causing moisture to be retained in the sensor resulting in a moist difference with the opposite happening for descending aircraft. The different radiosonde models that the NWS operates shows differences as well when compared with the WVSS-II. The CONUS average is shaped by the Lockheed Martin Sippican radiosonde model, which comprises 80% of the dataset. The Vaisala radiosondes comparisons show the WVSS-II being slightly dry in the lowest levels up to approximately 800 hPa. The seasons for the Lockheed Martin Sippican radiosonde followed the CONUS seasons where the Vaisala seasons have the continued dry difference in the lowest levels with the largest moist

difference in summer similar to the CONUS summer season. Higher level comparisons were made as well for the pressure range of 700 – 200 hPa. This pressure range showed the continued moist difference similar to the lowest levels with increased in variability above 300 hPa which appears to be caused by the poor response of the relative humidity sensor in temperatures below -40°C.

In addition to investigating how the WVSS-II preforms CONUS-wide, different climate regions were compared to examine how the sensor responds regions with different water vapor contents. Comparing all the regions together showed the largest variability at the lowest levels with agreement as altitude increased. Overall though, these individual regions followed the CONUS trend of the WVSS-II being slightly moister compared to the radiosondes. Examining two individual locations also showed the overall moist trend for Tampa Bay, FL but only in the mid-levels for Las Vegas, NV where a slight dry difference was present at the lowest-levels.

Examining the UPS aircraft separately showed the WVSS-II aboard UPS aircraft to be drier than the radiosondes below 850 hPa, nearly zero from 850 hPa to 700 hPa, and similar to the non-UPS aircraft above 700 hPa. The ascending observations from the UPS aircraft followed similarly to the non-UPS aircraft but the descending observations were drier than the radiosondes below 600 hPa. The time of day the observations were made did not appear to change the difference profiles for UPS or non-UPS aircraft.

The WVSS-II observations from one UPS aircraft for an entire year still showed the WVSS-II being moister at the lower and upper levels but showing nearly no difference in the mid-levels. Ascending and descending observations shows the descending observations having a smaller difference below 700 hPa with a spike in differences between 600 hPa and

550 hPa. This large difference could be due one set of bad observations since there is only one observation per 10 hPa layer.

Observations that originate from aircraft flying through precipitation was found to be a contributor to the moist difference throughout the CONUS average of differences. When aircraft fly through precipitation the difference between the WVSS-II observation and the radiosonde is approximately 1 g kg^{-1} greater than when it is clear regardless of pressure level. Because there is no countering dry difference to average out this much stronger moist difference, when all cases from the entire CONUS for an entire year are averaged together, precipitation and clear, overall there is a moist difference.

Contributing factors to differences between the WVSS-II observation and the radiosondes are the fact the moisture is highly variable within the atmosphere and even within 50 km, 10 hPa, and 30 minutes, there could be a moisture gradient that the radiosonde and WVSS-II are sampling differently. The WVSS-II also responds at a much faster rate than the radiosondes which could explain differences as well.

Overall, the WVSS-II shows good agreement when compared with radiosondes. Observations from this instrument have already been impactful for forecasters and for NWP. Continued deployment of this instrument would allow further gap-filling in the upper air observing network, greater NWP skill, and enhanced benefits for the aviation community, all for substantially less cost and greater accuracy than expanding the radiosonde network.

5.1 Future Work

Possible future work includes examining the precipitating cases versus the clear day cases throughout the CONUS for multiple seasons instead of at just one location for one season. This could be completed by using the already available Meteorological Terminal Aviation Routine Weather Report (METAR) and operational satellite cloud masks to determine the conditions a particular airplane is flying through.

To investigate the moisture variability in more depth, the examination of the differences of temporal and spatial distance between the WVSS-II observations and the radiosondes should be completed to see how the differences between the WVSS-II and radiosondes change. For example, one could reduce the number of allowable matches by reducing the spatial and temporal extent of the comparison criteria and evaluating how the differences change. This would confirm whether or not the current differences are due to sampling different moisture environments. Also, because the WVSS-II sensor is on two different types of aircraft, Boeing 757s and Boeing 737s, it is important to examine how the differences between the WVSS-II and radiosondes differ for these types of aircraft due to their flight patterns or where the sensor is located on the aircraft.

Gaining a thorough understanding of how the WVSS-II performs in all conditions allows for corrections to be made and confidence to be gained in the sensor, which in turn helps make the case that deployment of the WVSS-II across the nation's commercial fleet should be increased.

References

- Ballish, B. A. and V. K. Kumar, 2008: Systematic differences in aircraft and rawinsonde temperatures – Implications for NWP and climate studies. *Bull. Amer. Meteor. Soc.*, **89**, 1689-1707, doi:10.1175/2008BAMS2332.1.
- Bell, R. S., 1994: The beneficial impact of changes to observations usage in the U. K. Meteorological Office Operational Data Assimilation system. Preprints, *10th Conf. on Numerical Weather Prediction*, Portland, OR, Amer. Meteor. Soc., 485-487.
- DiMego, G. J., K. E. Mitchell, R. A. Petersen, J. E. Hoke, J. P. Gerrity, J. J. Tuccillo, R. L. Wobus, and H.-M. H. Juang, 1992: Changes to NMC's regional analysis and forecast system. *Wea. Forecasting*, **7**, 185-198.
- Drüe, C., T. Hauf, and A. Hoff, 2010: Comparison of Boundary-Layer Profiles and Layer Detection by AMDAR and WTR/RASS at Frankfurt Airport. *Boundary-Layer Meteor.*, **135**, 407-432, doi:10.1007/s10546-010-9485-0.
- Earth System Research Laboratory Global Systems Division, 2016: Aircraft Meteorological Data Reports (AMDAR) and Aircraft Communications Addressing and Reporting System (ACARS). Provided by NCAR/EOL under sponsorship of the National Science Foundation. <http://data.eol.ucar.edu/>.
- Fein, J. S., P. L. Stephens, and K. S. Loughran, 1983: The Global Atmospheric Research Program: 1979 – 1982. *Rev. Geophys.*, **21**(5), 1076–1096, doi:10.1029/RG021i005p01076.
- Fleming, R. J., T. M. Kaneshige, and W. E. McGovern, 1979: The Global Weather Experiment 1. The observational phase through the first special observing period. *Bull. Amer. Meteor. Soc.*, **60**, 649-661, doi: 10.1175/1520-0477(1979)060<0649:TGWETO>2.0.CO;2.
- Fleming, R. J., 1996: The use of commercial aircraft as platforms for environmental measurements. *Bull. Amer. Meteor. Soc.*, **77**, 2229-2242.
- Fleming, R. J., 2000: Water vapor measurements from commercial aircraft: Progress and plans. Preprints, Fourth Symp. On Integrated Observing Systems, Long Beach, CA, *Amer. Meteor. Soc.*, 30-33.

- Fleming, R. J., D. R. Gallant, W. F. Feltz, J. G. Meitin, W. R. Moninger, S. F. Williams, and R. T. Baker, 2002: Water vapor profiles from commercial aircraft. UCAR Rep., 37 pp. [Available online at <http://mailman.eol.ucar.edu/system/files/watervapor2.pdf>.]
- Fleming, R. J. and R. D. May 2004: The 2nd Generation Water Vapor Sensing System and Benefits of Its Use on Commercial Aircraft for Air Carriers and Society, 16 pp. [Available online at www.eol.ucar.edu/system/files/spectrasensors.pdf.]
- Giraytys, J., R. Deckter, G. Smidt, and J. Sparkman, 1981: Aircraft Meteorological Data Relay (AMDAR). *Proc. First Int. Conf. on Aviation Weather System*, Montreal, QC, Canada, Amer. Meteor. Soc., 135-145.
- Hartung, D. C., J. A. Otkin, R. A. Petersen, D. D. Turner, and W. F. Feltz, 2011: Assimilation of surface-based boundary layer profiler observations during a cool-season weather event using an Observing System Simulation Experiment. Part II: Forecast assessment. *Mon. Wea. Rev.*, **139**, 2327-2346, doi:10.1175/2011MWR3623.1.
- Helms, D., Hoff, A., Smit, H., Taylor, S. and Carlberg, S., 2010: Advancements in the AMDAR Humidity Sensing, WMO Technical Conference on Meteorological and Environmental Instruments and Methods of Observations, TECO-2010 Session 2, Aug 2010, Helsinki, Finland.
- Hoff, A. 2009: WVSS-II Assessment at the DWD. Deutscher Wetterdienst, 13 pp. [Available online at http://amdar.noaa.gov/docs/WVSS-II_Assessment_DWD.pdf.]
- Hughes, P. and D. Gedzelman, 1995: The new meteorology. *Weatherwise*. **48**, 26-36.
- Jamison, B., and W. R. Moninger, 2002: An analysis of the temporal and spatial distribution of ACARS data in support of the TAMDAR program. Preprints, 10th conference on Aviation, Range, and Aerospace Meteorology, Portland, OR, *Amer. Meteor. Soc.*, J33-J36.
- Kottek, M., J. Grieser, C. Beck, B. Rudolf, and F. Rubel, 2006: World Map of the Köppen-Geiger climate classification updated. *Meteorol. Z.*, **15**, 259-263. DOI: 10.1127/0941-2948/2006/0130.
- Langland, R. H. and N. L. Baker, 2004: Estimation of observation impact using the NRL atmospheric variational data assimilation adjoint system. *Tellus*, **56A**, 3, 189 – 201.

- Lord, R. J., W. P. Menzel, and L. E. Pecht, 1984: ACARS wind measurements: An intercomparison with radiosonde, cloud motion, and VAS thermally derived winds. *J. Atmos. Oceanic Technol.*, **1**, 131-137.
- Mamrosh, R., Gillis, J., Petersen, R., and Baker, R.: A Comparison of WVSS-II and NWS Radiosonde Temperature and Moisture Data, 10th Symposium on Integrated Observing and Assimilation Systems for the Atmosphere, Oceans, and Land Surface (IOAS-AOLS), Atlanta, GA, 28 January–2 February 2006, available at: <https://ams.confex.com/ams/pdfpapers/104889.pdf>
- Martin, R. C., M. M. Wolfson, and R. G. Hallowell, 1993: MDCRS: Aircraft observations collection and uses. Preprints, *Fifth Conf. on Aviation Weather*, Vienna, VA, Amer. Meteor. Soc., 317-321.
- Mati, I., Sarrazin, R., Zaitseva, Y., and Verner, G., 2009: Monitoring and Assimilation Impact Study of Moisture Data from Aircraft at the Canadian Meteorological Center. 3th Conference on Integrated Observing and Assimilation Systems for Atmosphere, Oceans, and Land Surface (IOAS-AOLS), January 10 - 16, Phoenix, AZ, USA.
- Moninger, W. R. , R. D. Mamrosh, and P. M. Pauley, 2003: Automated meteorological reports from commercial aircraft, *Bulletin of the American Meteorological Society*. *Amer. Meteor. Soc.*. 203-216.
- NOAA National Weather Service Radiosonde Observations: Upper Air Factsheet. Accessed Nov. 29 2016. [Available at <http://www.ua.nws.noaa.gov/factsheet.htm>.]
- Otkin, J. A., D. C. Hartung, D. D. Turner, R. A. Petersen, W. F. Feltz, and E. Janzon, 2011: Assimilation of surface-based boundary layer profiler observations during a cool-season weather event using an Observing System Simulation Experiment. Part I: Analysis impact. *Mon. Wea. Rev.*, **139**, 2309-2326, doi:10.1175/2011MWR3622.1.
- Petty, G. W., 2008: *A First Course in Atmospheric Thermodynamics*. Sundog Publishing, 338 pp.
- Petersen, R. A., W. Feltz, E. Olson, and S. Bedka, 2006: Evaluation of the WVSSII Moisture Sensor Using Co-Located In-Situ and Remotely Sensed Observations. *10th Symp. On Integrated Observing and Assimilation Systems for the Atmosphere, Oceans, and Land Surface (IOAS-AOLS)*, Atlanta, GA, Amer. Meteor. Soc., P2.6. [Available online at http://ams.confex.com/ams/Annual2006/techprogram/paper_102987.htm.]

- Petersen, R., and W. R. Moninger 2006: Assessing two different commercial aircraft-based sensing systems. 10th Symposium on Integrated Observing and Assimilation Systems for the Atmosphere, Oceans, and Land Surface, Atlanta, GA, *Amer. Meteor. Soc.*.
- Petersen, R. A., L. M. Crouce, W. F. Feltz, E. Olson, and D. Helms, 2011: Validation studies of WVSS-II Moisture Observations. 15th Symp. On Integrated Observing and Assimilation Systems for the Atmosphere, Oceans, and Land Surface (IOAS-AOLS), Seattle, WA, Amer. Meteor. Soc., 209. [Available online at <https://ams.confex.com/ams/91Annual/webprogram/Paper184449.html>.]
- Petersen, R. A., 2016: On the impact and benefits of AMDAR observations in operational forecasting. Part I: A review of the impact of automated aircraft wind and temperature reports. *Bull. Amer. Meteor. Soc.*, **97**, 585–602, doi: 10.1175/BAMS-D-14-00055.1.
- Petersen, R. A., L. M. Crouce, R. Mamrosh, R. Baker, and P. Pauley, 2016b: On the impact and future benefits of AMDAR observations in operational forecasting - Part 2: Water Vapor Observations. *Bull. Amer. Meteor. Soc.*, #, doi: 10.1175/BAMS-D-14-00211.1.
- Rahn, D. and C. Mitchell, 2016: Diurnal Climatology of the Boundary Layer in Southern California Using AMDAR Temperature and Wind Profiles. *J. Appl. Meteor. Climatol.*, **55**, 1123–1137, doi: 10.1175/JAMC-D-15-0234.1.
- Schwartz, B. and S. G. Benjamin, 1995: A Comparison of Temperature and Wind Measurements from ACARS-Equipped Aircraft and Rawinsondes. *Wea. Forecasting*, **10**, 528-544.
- Sparkman, J. K., J. Giraytys, and G. J. Smidt, 1981: ASDAR: A FGGE real-time data collection system. *Bull. Amer. Meteor. Soc.*, **62**, 394-400.
- Spectra Sensors, 2010: Atmospheric Water Vapor Sensing System (WVSS) technical specifications. Spectra Sensors, 4 pp. [Available online at www.spectrasensors.com/files/525/.]
- Sun, B., A. Reale, S. Schroeder, D. J. Seidel, and B. Ballish (2013), Toward improved corrections for radiation-induced biases in radiosonde temperature observation, *J. Geophys. Res. Atmos.*, **118**, 4231 – 4243, doi: 10.1002/jgrd.50369.

- Vaisala, 2015: Vaisala Radiosonde RS92-SGP. Vaisala, 2 pp. [Available online at www.vaisala.com/Vaisala%20Documents/Brochures%20and%20Datasheets/RS92SGP-Datasheet-B210358EN-F-LOW.pdf.]
- Vömel, H., H. Selkirk, L. Miloshevich, J. Valverde-Canossa, J. Valdés, E. Kyrö, R. Kivi, W. Stolz, G. Peng, and J. Diaz, 2007: Radiation Dry Bias of the Vaisala RS92 Humidity Sensor. *J. Atmos. Oceanic Technol.*, 24, 953–963, doi: 10.1175/JTECH2019.1.
- Wang, J., L. Zhang, A. Dai, F. Immler, M. Sommer, and H. Vömel, 2013: Radiation dry bias correction of Vaisala RS92 humidity data and its impacts on historical radiosonde data. *J. Atmos. Oceanic Technol.*, 30, 197–214, doi:10.1175/JTECH-D-12-00113.1.
- Wendisch, M., and J.-L. Brenguier, Eds., 2013: *Airborne Measurements for Environmental Research: Methods and Instruments*. Wiley-VCH, 641 pp.
- WMO, 2003: Aircraft Meteorological Data Relay (AMDAR) reference manual. World Meteorological Organization, 84 pp.
- WMO, 2014a: WIGOS WMO Integrated Global Observing System: Requirements for the implementation and operation of an AMDAR programme. WMO Tech. Rep. 2014-2, 31 pp.
- WMO, 2014b: WIGOS WMO Integrated Global Observing System: The Benefits of AMDAR Data to Meteorology and Aviation. WIGOS Tech Report 2014-01, 47 pp.
- Zhu, Y., J. Derber, R. J. Purser, J. Whiting, and B. A. Ballish, 2015: Variational correction of aircraft temperature bias in the NCEP's GSA analysis system. *Mon. Wea. Rev.*, **143**, 3774-3803, doi: 10.1175/MWR-D-14-00235.1.